

**Performance Evaluation of 24 Ion Exchange
Materials for Removing Cesium and
Strontium from Actual and Simulated
N-Reactor Storage Basin Water**

G. N. Brown
K. J. Carson
J. R. DesChane
R. J. Elovich

September 1997

DISTRIBUTION OF THIS DOCUMENT IS UNLIMITED *ph*

Prepared for
the U.S. Department of Energy
under Contract DE-AC06-76RLO 1830

MASTER

Pacific Northwest National Laboratory
Richland, Washington 99352

DISCLAIMER

Portions of this document may be illegible in electronic image products. Images are produced from the best available original document.

DISCLAIMER

This report was prepared as an account of work sponsored by an agency of the United States Government. Neither the United States Government nor any agency thereof, nor any of their employees, makes any warranty, express or implied, or assumes any legal liability or responsibility for the accuracy, completeness, or usefulness of any information, apparatus, product, or process disclosed, or represents that its use would not infringe privately owned rights. Reference herein to any specific commercial product, process, or service by trade name, trademark, manufacturer, or otherwise does not necessarily constitute or imply its endorsement, recommendation, or favoring by the United States Government or any agency thereof. The views and opinions of authors expressed herein do not necessarily state or reflect those of the United States Government or any agency thereof.

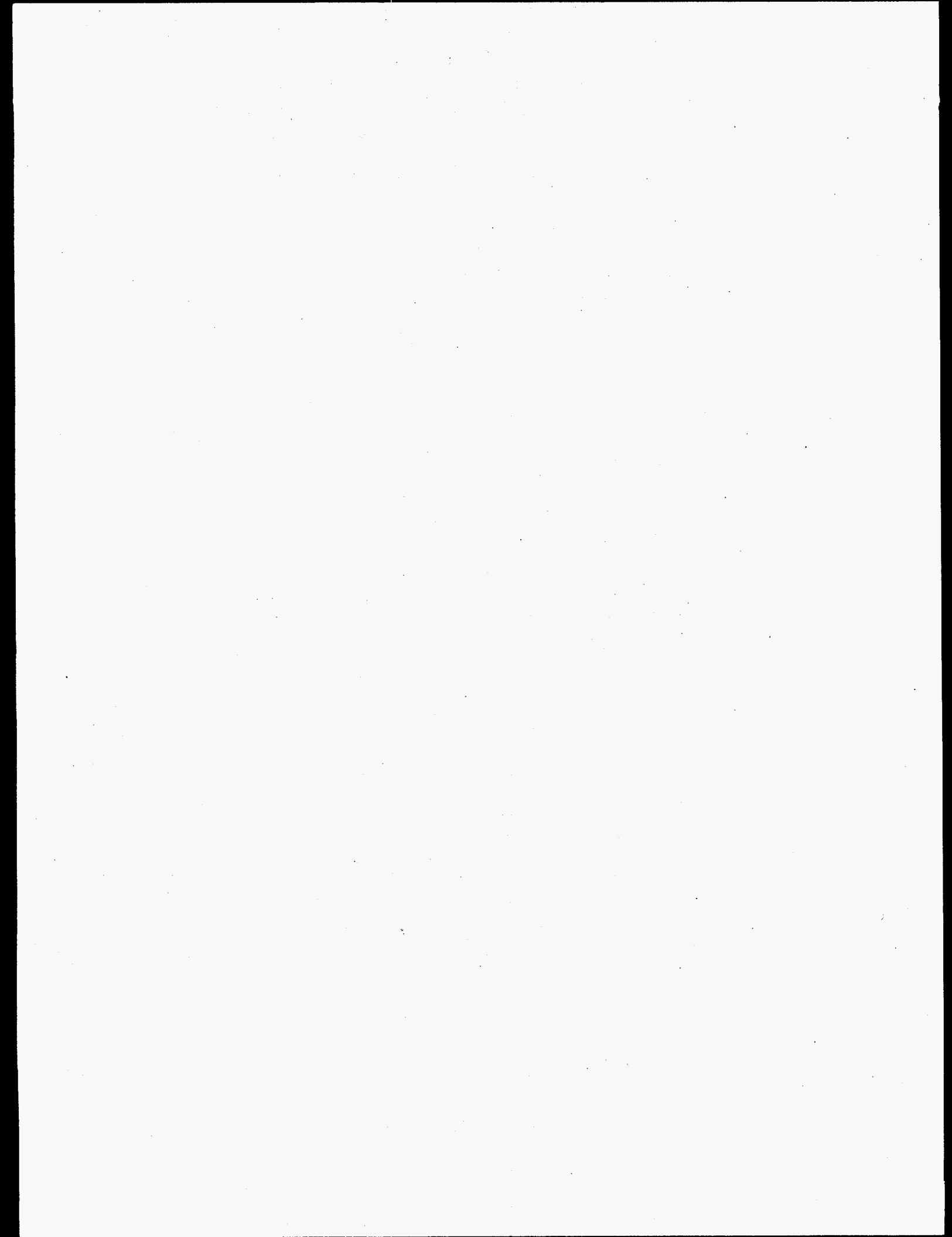
Abstract

This report describes the evaluation of 24 organic and inorganic ion exchange materials for removing cesium and strontium from actual and simulated waters from the 100 Area 105 N-Reactor fuel storage basin. The data described in this report can be applied for developing and evaluating ion exchange pre-treatment process flowsheets. Cesium and strontium batch distribution ratios (K_d 's), decontamination factors (DF), and material loadings (mmol g^{-1}) are compared as a function of ion exchange material and initial cesium concentration.

The actual and simulated N-Basin waters contain relatively low levels of aluminum, barium, calcium, potassium, and magnesium (ranging from $8.33\text{E-}04$ to $6.40\text{E-}05$ M), with slightly higher levels of boron ($6.63\text{E-}03$ M) and sodium ($1.62\text{E-}03$ M). The ^{137}Cs level is $1.74\text{E-}06$ Ci L^{-1} which corresponds to approximately $4.87\text{E-}10$ M Cs. The initial Na/Cs ratio was $3.33\text{E+}06$. The concentration of total strontium is $4.45\text{E-}06$ M , while the ^{90}Sr radioactive component was measured to be $6.13\text{E-}06$ Ci L^{-1} . Simulant tests were conducted by contacting 0.067 g or each ion exchange material with approximately 100 mL of either the actual or simulated N-Basin water. The simulants contained variable initial cesium concentrations ranging from $1.00\text{E-}04$ to $2.57\text{E-}10$ M Cs while all other components were held constant.

For all materials, the average cesium K_d was independent of cesium concentration below approximately $1.0\text{E-}06$ M . Above this level, the average cesium K_d values decreased significantly. Cesium K_d values exceeding $1.0\text{E+}07$ mL g^{-1} were measured in the simulated N-Basin water. However, when measured in the actual N-Basin water the values were several orders of magnitude lower, with a maximum of $1.24\text{E+}05$ mL g^{-1} observed. Several materials, including a potassium cobalt hexacyanoferrate (KCoHex), inorganic zeolites, crystalline silicotitanates, biotite micas, pharmacosiderites, and phlogopites exhibited substantial affinity for cesium. The nonspecific cation exchange materials did not show an appreciable affinity for cesium in the basin water.

Because of the high levels of nonradioactive strontium and calcium, the strontium K_d results were much lower (e.g., between $1.0\text{E+}03$ and $1.0\text{E+}05$ mL g^{-1}) than those for the cesium. The strontium K_d and loading were inversely correlated to the cesium concentration (increasing with decreasing concentration from $1.0\text{E-}04$ to $1.0\text{E-}09$ M Cs). The data suggest that either the two ions compete for similar ion exchange sites or the higher cesium loading perturbs the strontium sites such that the strontium exchange process is hindered.



Summary

This report describes evaluations of the radionuclide uptake capability of several newly produced ion exchange materials under actual waste solution conditions and compares the results obtained with these materials to those obtained with other commercial and experimental exchangers. The ion exchange materials are being evaluated for their performance in treating water from the 105 N-Reactor basin at Hanford. Actual and simulated basin water was used in this work.

A number of organic and inorganic exchangers are being or have been developed and evaluated for removing ^{137}Cs , ^{90}Sr , and other radionuclides from Hanford tank wastes. Many of these materials, although targeted for use with highly alkaline tank wastes, also may be capable of removing cesium and strontium from more neutral pH process and ground waters. The exchangers investigated in this work include materials produced on an experimental basis by AlliedSignal (biotites); Texas A&M University (pharmacosiderites, phlogopites, biotites), and 3M (potassium cobalt hexacyanoferrates). In addition, some commercial materials were tested, including several versions of the crystalline silicotitanate (CST) sorbent developed by Sandia National Laboratories/Texas A&M and produced commercially by UOP [powdered IONSIV® IE-910, referred to as IE-910; and three batches of engineered IONSIV® IE-911, referred to as IE-911 (08), IE-911 (38B), and IE-911 (999)]; a resorcinol-formaldehyde (R-F) polymer developed at Westinghouse Savannah River Company and produced by Boulder Scientific; two inorganic zeolite exchangers produced by UOP (IONSIV® TIE-96 and IONSIV® IE-96, referred to as TIE-96 and IE-96); a macrocyclic organic resin developed and produced by IBC Advanced Technologies (SuperLig® 644, referred to as SL-644); several Amberlite™ resins (IRC-76, IRC-718, CG-120, and C-467) produced by Rohm & Haas; and clinoptilolite, an inexpensive natural zeolite. Many of these materials are still under development and may not necessarily be in their optimal form.

The data described in this report can be applied for developing and evaluating ion exchange pretreatment process flowsheets. Cesium and strontium batch distributions ratios (K_d 's), column distribution ratios ($\delta = K_d \times D_b$), decontamination factors (DF), and material loadings (mmol g^{-1}) are compared as a function of ion exchange material and initial cesium concentration. The actual and simulated N-Basin waters contain relatively low levels of aluminum, barium, calcium, potassium, and magnesium (ranging from $8.33\text{E-}04$ to $6.40\text{E-}05 \text{ M}$), with slightly higher levels of boron ($6.63\text{E-}03 \text{ M}$) and sodium ($1.62\text{E-}03 \text{ M}$). The ^{137}Cs level is $1.74\text{E-}06 \text{ Ci L}^{-1}$ which corresponds to approximately $4.87\text{E-}10 \text{ M Cs}$. The initial Na/Cs ratio was $3.33\text{E+}06$. The concentration of total strontium is $4.45\text{E-}06 \text{ M}$ while the ^{90}Sr radioactive component was measured to be $6.13\text{E-}06 \text{ Ci L}^{-1}$. Simulant tests were conducted using a stock solution with a variable initial cesium level ranging from $1.00\text{E-}04$ to $2.57\text{E-}10 \text{ M Cs}$ while holding all other components constant. Following are specific conclusions and recommendations from the study:

- As a general trend, the average cesium K_d of each material was independent of the cesium concentration below approximately $1.0\text{E-}06 \text{ M}$. However, between $1.0\text{E-}06$ and $1.0\text{E-}04 \text{ M Cs}$, the average cesium K_d values decreased significantly.

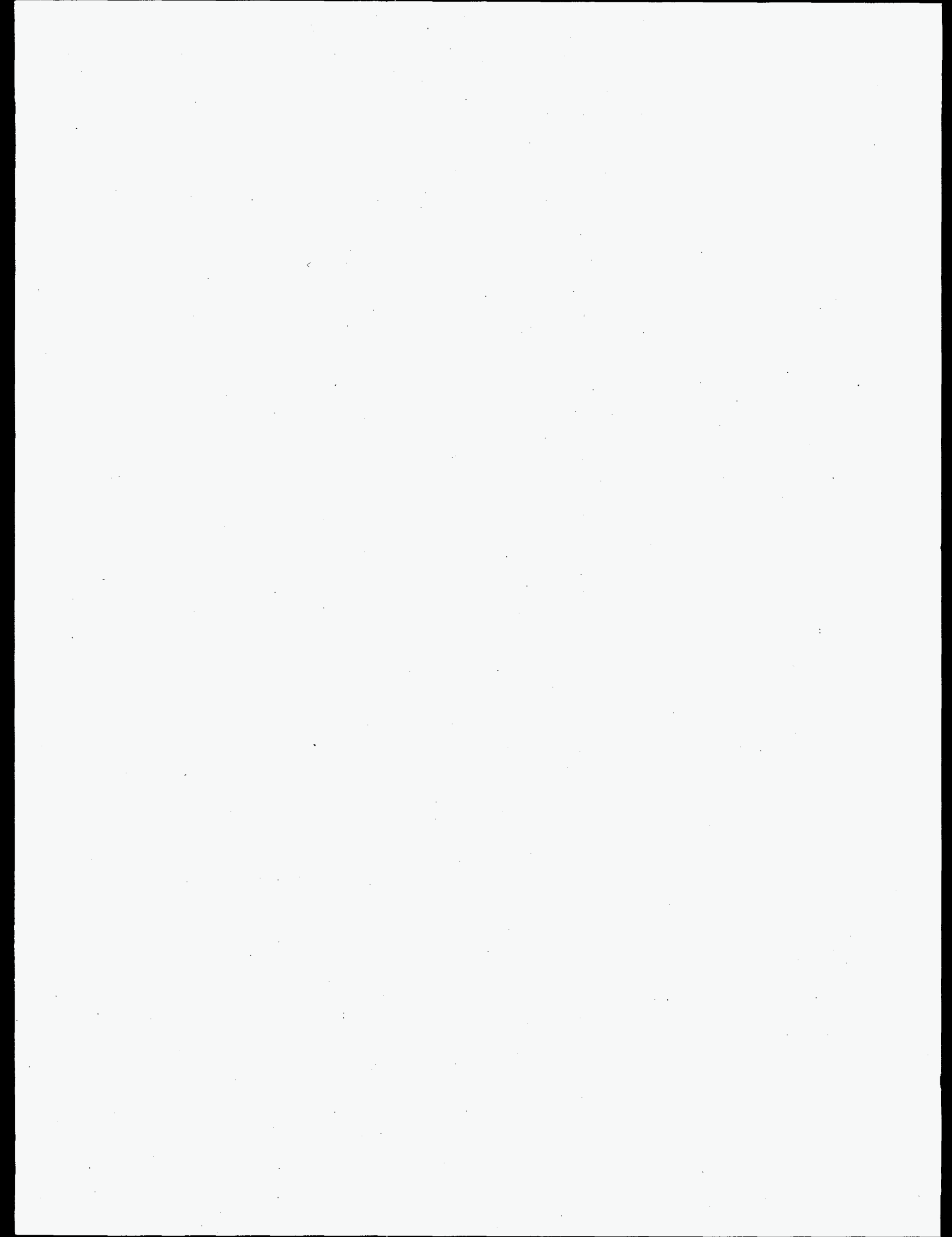
- Average cesium K_d values exceeding $1.0E+07$ mL g⁻¹ were measured in the simulated N-Basin water. Several materials, including potassium cobalt hexacyanoferrate, crystalline silicotitanates, biotite micas, pharmacosiderites, and phlogopites exhibited substantial cesium uptake.
- The cesium K_d values in the actual N-Basin water were lower, in certain cases by several orders of magnitude, than those obtained from the simulated solutions. In the actual water, a maximum cesium K_d value of $1.24E+05$ mL g⁻¹ (e.g., an AlliedSignal modified biotite mica) was recorded.
- Nonspecific cation exchange materials (e.g., Duolite C-467, Amberlite IRC-76, IRC-718) and certain materials that are selective for cesium in highly caustic solutions (e.g., SuperLig® 644, resorcinol-formaldehyde) did not show an appreciable affinity for cesium in the basin water.
- Because of the high levels of nonradioactive strontium and calcium, the strontium K_d results were much lower (e.g., between $1.0E+03$ and $1.0E+05$ mL g⁻¹) than the cesium K_d results. In general, the inorganic materials (e.g., TSP-137, pharmacosiderite, crystalline silicotitanates) showed the best strontium removal performance.
- Similar to the cesium results, the strontium K_d values in the actual N-Basin water were lower than those obtained from the simulated solutions. The differences were mostly insignificant except with the highest performance materials, where a discrepancy of a factor of ten was observed. In the actual water, a maximum strontium K_d value of $3.26E+04$ mL g⁻¹ (e.g., TSP-137 produced by Texas A&M) was recorded.
- The strontium K_d and loading were inversely correlated to the cesium concentration (increasing with decreasing concentration from $1.0E-04$ to $1.0E-09$ M Cs). The data suggest that either the two ions compete for similar ion exchange sites or the higher cesium loading perturbs the strontium sites such that the strontium exchange process is hindered.

Acknowledgments

Pacific Northwest National Laboratory (PNNL) is collaborating with universities, national laboratories, and industry to develop and test new materials for pretreating nuclear wastes stored at the Hanford site. The experimental work described in this report would not have been possible without the encouragement and resources provided by the Office of Environmental Restoration and Waste Management's Office of Science and Technology of the U.S. Department of Energy (DOE) and the Efficient Separations and Processing Cross Cutting Program (ESP).

The work described in this report was performed by researchers at PNNL under ESP's Technical Task Plan (TTP) RL3-6-C3-42. PNNL is operated for the U.S. Department of Energy by Battelle under Contract DE-AC06-76RLO 1830. Technical peer review was provided by J. R. Bontha, I. E. Burgeson, and C. D. Carlson (PNNL).

The authors would like to acknowledge the contributions to this effort of W. F. Bonner and W. L. Kuhn at PNNL (Richland, WA) for programmatic support; L. A. Bray (retired) for technical support and mentoring; P. K. Berry, S. K. Fadeff, M. W. Goheen, L. R. Greenwood, M. M. O'Neill, K. A. Poeppel, R. T. Ratner, D. R. Sanders, R. T. Steele, J. J. Wagner, and M. W. Urie at PNNL for analytical support; G. E. Johnson and M. R. Telander at PNNL for cobalt-60 irradiation of various materials; K. J. Carson, J. R. DesChane, and R. J. Elovich at PNNL for ion exchange material evaluations; D. Boggs, K. Carlson, T. Fredrickson, T. Kafka, D. C. Seely, I. Shaw-Epperson, N. Stern, L. R. White, and E. Wisted at 3M (St. Paul, MN) for the development of the web technology and potassium cobalt hexacyanoferrate materials; R. L. Bruening, R. H. Decker, S. R. Izatt, G. Maas, and B. Tarbet at IBC Advanced Technologies (American Fork, UT) for the development and production of the SuperLig® 644 ligand technology; S. F. Yates, R. Gaita, R. Sedath, and I. C. Gangi-DeFilippi for developments in the engineering of inorganic ion exchangers; Professor Abraham Clearfield, A. I. Bortun, L. M. Bortun, E. A. Behrens, and D. M. Poojary at Texas A&M University for the development of new and emerging inorganic ion exchange materials; J. P. Bibler (deceased) and R. M. Wallace at the Westinghouse Savannah River Company (WSRC) for development of the resorcinol-formaldehyde resin (R-F); N. E. Brown (retired), R. G. Dosch (deceased), and J. E. Miller at Sandia National Laboratories (SNL) for development and testing of the crystalline silicotitanate (CST); and Professor R. G. Anthony, Texas A&M, for development and modeling of the CST material. The engineered CST (IONSIV® IE-911) was developed by UOP, Des Plaines, Illinois, under a Cooperative Research and Development Agreement (CRADA) with SNL.



Contents

| | |
|--|-----|
| Abstract | iii |
| Summary | v |
| Acknowledgments | vii |
| 1.0 Introduction..... | 1.1 |
| 1.1 Decontamination Requirements | 1.1 |
| 1.2 Objectives..... | 1.2 |
| 1.3 Scope | 1.3 |
| 1.4 Strategy..... | 1.3 |
| 2.0 Experimental Approach | 2.1 |
| 2.1 Batch Distribution Coefficient | 2.1 |
| 2.2 Material Selection and Preparation | 2.3 |
| 2.3 Waste Composition and Preparation..... | 2.6 |
| 2.4 Simulant Test Conditions..... | 2.8 |
| 2.5 Actual Waste Test Conditions..... | 2.8 |
| 3.0 Results and Discussion | 3.1 |
| 3.1 Simulated N-Basin Water Results..... | 3.1 |
| 3.1.1 Cesium Batch Distribution | 3.1 |
| 3.1.2 Cesium Loading..... | 3.4 |
| 3.1.3 Strontium Batch Distribution..... | 3.7 |
| 3.1.4 Strontium Loading..... | 3.8 |

| | |
|--|------|
| 3.1.5 Cesium Dependence on Strontium Results | 3.10 |
| 3.2 Actual Waste Results | 3.10 |
| 3.2.1 Cesium Batch Distribution | 3.10 |
| 3.2.2 Strontium Batch Distribution..... | 3.11 |
| 3.3 Comparison of Simulated and Actual Waste Results | 3.13 |
| 3.3.1 Cesium Batch Distribution | 3.13 |
| 3.3.2 Strontium Batch Distribution..... | 3.14 |
| 4.0 Conclusions..... | 4.1 |
| 5.0 References..... | 5.1 |
| Appendix A - Data Set for All Materials Tested..... | A.1 |

Figures

| | | |
|------|--|------|
| 3.1 | Average Batch Distribution Coefficients for Cesium as a Function of Equilibrium Cesium Concentration for 24 Ion Exchange Materials in Simulated 105 N-Basin Water..... | 3.1 |
| 3.2 | Average Cesium Batch Distribution Coefficients for Cesium as a Function of Equilibrium Cesium Concentration for Selected Ion Exchange Materials in Simulated 105 N-Basin Water | 3.3 |
| 3.3 | Average Cesium Loading as a Function of Equilibrium Cesium Concentration for 24 Ion Exchange Materials in Simulated 105 N-Basin Water | 3.4 |
| 3.4 | Average Cesium Loading as a Function of Equilibrium Cesium Concentration for 24 Ion Exchange Materials in Simulated 105 N-Basin Water | 3.5 |
| 3.5 | Average Cesium Loading as a Function of Equilibrium Cesium Concentration for Selected Ion Exchange Materials in Simulated 105 N-Basin Water | 3.6 |
| 3.6 | Average Batch Distribution Coefficients for Strontium as a Function of Equilibrium Strontium Concentration for 24 Ion Exchange Materials in Simulated 105 N-Basin Water..... | 3.7 |
| 3.7 | Average Strontium Loading as a Function of Equilibrium Strontium Concentration for 24 Ion Exchange Materials in Simulated 105 N-Basin Water | 3.8 |
| 3.8 | Average Strontium Loading as a Function of Equilibrium Strontium Concentration for 24 Ion Exchange Materials in Simulated 105 N-Basin Water | 3.9 |
| 3.9 | Average Batch Distribution Coefficients for Strontium as a Function of the Equilibrium Cesium Concentration for Selected Ion Exchange Materials in Simulated 105 N-Basin Water..... | 3.10 |
| 3.10 | Average Strontium Loading as a Function of Equilibrium Cesium Concentration for Selected Ion Exchange Materials in Simulated 105 N-Basin Water | 3.11 |
| 3.11 | Comparison of Average Batch Distribution Coefficients for Cesium for 24 Ion Exchange Materials in Actual and Simulated 105 N-Basin Water..... | 3.14 |
| 3.12 | Comparison of Average Cesium Loadings for 24 Ion Exchange Materials in Actual and Simulated 105 N-Basin Water | 3.15 |

| | | |
|------|---|------|
| 3.13 | Comparison of Average Batch Distribution Coefficients for Strontium for 24 Ion Exchange Materials in Actual and Simulated 105 N-Basin Water | 3.15 |
| 3.14 | Comparison of Average Strontium Loadings for 24 Ion Exchange Materials in Actual and Simulated 105 N-Basin Water | 3.16 |

Tables

| | | |
|-----|---|------|
| 2.1 | Selected Physical Properties of Cesium and Strontium Selective Materials | 2.4 |
| 2.2 | Chemical Composition of the 105 N-Basin Water | 2.6 |
| 2.3 | Chemical Composition of the Simulated 105 N-Basin Water | 2.7 |
| 2.4 | Simulant Testing Conditions | 2.8 |
| 3.1 | Summary of Averaged Cesium Batch Distribution Results from Actual 105 N-Basin Water | 3.12 |
| 3.2 | Summary of Averaged Strontium Batch Distribution Results from Actual 105 N-Basin Water | 3.13 |

1.0 Introduction

The N Reactor is one of several nonoperating reactors formerly operated by the U.S. Department of Energy (DOE). It is located in the 100 Area of DOE's Hanford Site, along the Columbia River approximately 30 miles north of Richland, Washington. The reactor is currently shut down and will require eventual decontamination and decommissioning (D&D). Water from fuel storage basins in the reactor also must be treated, as directed by the *Hanford Federal Facility Agreement and Consent Order* (Tri-Party Agreement) milestone M-16-01E-T2, which requires initiating the pretreatment and removal of all N Reactor fuel storage basin waters pursuant to the N Reactor Deactivation Program Plan. Pretreatment and removal of the N-Basin water is a prerequisite for overall deactivation and decommissioning of the N Reactor facility.

One of the fuel storage basins in the N Reactor facility, the 105-N fuel storage pool (N-Basin), contains approximately one million gallons of virtually pure water contaminated with trace quantities of radioactive ^{137}Cs , ^{90}Sr , and ^{60}Co , as well as minor quantities of $^{154/155}\text{Eu}$, ^{241}Am , and ^3H . The basin contains about 23 curies of dissolved ^{90}Sr at a concentration of 6.13 microcuries per liter ($\mu\text{Ci L}^{-1}$) and 6.6 curies of dissolved ^{137}Cs at a concentration of $1.74 \mu\text{Ci L}^{-1}$. Except for tritium, no other dissolved radionuclides are present in concentrations exceeding $0.0053 \mu\text{Ci L}^{-1}$. Cobalt-60 is present at approximately $0.0012 \mu\text{Ci L}^{-1}$ as suspended solids and can be removed by simple filtration. The basin water contains only minimal amounts of nonradioactive species (part per million levels of chloride, bromide, nitrate, and sulfate with a total conductivity of $300 \mu\text{mho}$).

Extensive evaluation of various options for treating storage basin waters has already been completed (Greenidge 1995; Hunacek 1992). This report describes experimental evaluations of inorganic ion exchangers for removing cesium and strontium from the waters.

1.1 Decontamination Requirements

Although the pretreatment and disposal requirements for the 105 N-Basin water are still being defined, one of the first steps in most pretreatment scenarios will be to retrieve residual equipment, debris, and miscellaneous large materials from the bottom of the basin. The second step probably will be filtration of the pumpable waste water to separate and remove residual algae, colloidal cobalt-60, suspended particulate, and sediment. Most of the radioactive cesium and strontium contamination that accumulates in the water as a result of these processes is expected to remain in the basin water. These contaminants must be removed to reduce radiation exposure to facility operations personnel and achieve the waste disposition requirements. Methods to remove those contaminants are the focus of the current ion exchange batch distribution experiment. The removal methods are being designed to remove cesium and strontium to levels below drinking water standards. The basin water will likely require a decontamination factor of close to one million.

Because the basin water contains several radionuclides besides ^{137}Cs and ^{90}Sr at concentrations exceeding federal drinking water standards, additional pretreatment may be required before the water's final discharge to the environment. Fong and Hyman (1995) concluded that the recommended disposal method is to use minimal pretreatment in order to sufficiently reduce the radioactive inventory for acceptance of the water at the Effluent Treatment Facility (ETF) in the 200 East Area, or its possible disposal to the soil column or the Columbia River. Greenidge (1995) and Hunacek (1992) suggest that final treatment either at the ETF or N Reactor facility likely will include one or more of the following steps: prefiltration (hydrocyclone, deep bed, macro, micro, and ultra scales), flocculation (iron hydroxide, other inorganic compounds, or proprietary organic polyanionic surfactants), chemical oxidation (e.g., hydrogen peroxide, chlorine dioxide, potassium permanganate, etc.), short wavelength ultraviolet oxidation, standard ion exchange with possible polishing, reverse osmosis, and evaporation (e.g., solar pond, spray nozzle, evaporator) or final discharge/disposal (e.g., soil column, Columbia River, ETF).

However, other treatment alternatives are worth considering in case the ETF is not available to meet the schedule or additional pretreatment is needed to reduce the inventory of radioactive species to be handled at the ETF. Demonstration of another feasible treatment alternative could be of value for other fuel basins at Hanford and other DOE sites, and at commercial nuclear power plants.

1.2 Objectives

Experimental ion exchange studies are being conducted at the Pacific Northwest National Laboratory (PNNL)^(a) for the Efficient Separations and Processing Cross-Cutting Program (ESP) to evaluate newly emerging materials and technologies for removing radioactive cesium, strontium, cobalt, technetium, and transuranic elements (TRUs) from simulated and actual wastes at Hanford. Previous work focused on technologies for use with high-level alkaline tank wastes (HLW), but many of those technologies also find application in process and ground water remediation.

The primary goal of the work reported here was to evaluate experimental performance of several newly prepared inorganic ion exchangers and compare the results to those obtained with baseline and commercially available materials under identical conditions. The specific experimental objectives described in this report were to

1. determine cesium and strontium batch distribution coefficients, decontamination factors, and material loadings in actual Hanford 105 N-Basin water,
2. compare the performance of newly produced materials from AlliedSignal and Texas A&M with other commercial and baseline exchangers,
3. verify simulant performance, and

(a) Pacific Northwest National Laboratory (PNNL) is operated by Battelle Memorial Institute for the U.S. Department of Energy under Contract DE-AC06-76RLO 1830.

4. experimentally obtain generic ion exchange data under neutral pH conditions that can be applied to a broad range of process wastes.

1.3 Scope

The exchangers that were investigated in this work include chemically modified natural minerals and mineral analogs produced by AlliedSignal and Texas A&M (e.g., pharmacosiderite, biotite, phlogopite, sodium zirconium silicate, etc.); powdered (IONSIV® IE-910, referred to as IE-910) and engineered (IONSIV® IE-911, referred to as IE-911) forms of the crystalline silico-titanate (CST) inorganic sorbent developed by Sandia National Laboratories (SNL)/ Texas A&M and prepared by UOP; a phenol-formaldehyde (CS-100) resin developed by Rohm and Haas; a resorcinol-formaldehyde (R-F) polymer developed at the Westinghouse Savannah River Company (WSRC) and produced by Boulder Scientific; two inorganic zeolite exchangers produced by UOP (IONSIV® IE-96, referred to as IE-96 and IONSIV® TIE-96, referred to as TIE-96); and a macrocyclic organic resin developed and produced by IBC Advanced Technologies (SuperLig® 644, referred to as SL-644). Several of these materials are still under development and may not be in the optimal form.

1.4 Strategy

The experiments described in this report involve the direct comparison of several ion exchange materials for the pretreatment of actual and simulated Hanford 105 N-Basin water. The comparative parameters included radionuclide removal efficiency (decontamination factor, percent removal), batch distribution coefficient (K_d), and material loading (mmol g^{-1}) under a variety of solution conditions. The basic experimental operation involved batch contacts between the exchangers and the simulant or actual waste solutions. The advantage of batch testing relative to column testing is that a large amount of equilibrium data can be obtained with a relatively small amount of waste at reduced unit cost (i.e., cost per data point). Simulant tests were conducted over a broad range of cesium concentrations ($[\text{Cs}] = 1.00\text{E-}04, 1.00\text{E-}05, 1.00\text{E-}06, 1.00\text{E-}07, 1.00\text{E-}08, \text{ and } 2.74\text{E-}10 \text{ mol L}^{-1} (\text{M})$) to provide additional equilibrium data over a large number of experimental conditions and to compare the actual waste results to those obtained from the simulants.

2.0 Experimental Approach

The following sections briefly describe the experimental exchanger materials and the method of exchanger pretreatment, the actual and simulated waste solutions, and the experimental procedures that were used.

2.1 Batch Distribution Coefficient

Ion exchange is a classic method for the separation and/or removal of dissolved ions from a wide variety of solutions (Buckingham 1967; Samuelson 1953; Samuelson 1963). The batch distribution coefficient (K_d) is an equilibrium measure of the overall ability of the solid phase ion exchange material to remove an ion from solution under the particular experimental conditions that exist during the contact. The batch K_d is an indicator of the selectivity, capacity, and affinity of an ion exchange material for a particular ion in the presence of a complex matrix of competing ions. The addition of a small quantity of ion exchange material into a small volume of supernatant solution is an extremely rapid and cost-effective method for comparing a wide variety of such materials. By definition, this equilibrium method does not normally provide information about exchange kinetics but is useful for measuring equilibrium exchange under the particular conditions of the test. Accurate comparison of K_d results requires comparisons between tests conducted under identical experimental conditions (e.g., volume:mass ratio, equilibrium solution composition, material pretreatment, temperature) because all of the conditions are known to affect K_d .

In the standard batch K_d tests, a known quantity of ion exchange material is placed in contact with a known volume of waste. The material is allowed to contact the solution at constant temperature for sufficient time to reach equilibrium, after which the solid ion exchange material and liquid supernate are separated. The concentration of the species of interest is determined in the solution and in the solid phase. In practice, it is easier to measure the concentration of the ion of interest in the solution instead of in the solid. Therefore, the equation for determining the batch distribution can be simplified by determining the concentration of the analyte before and after contact and calculating the quantity of analyte on the ion exchanger by difference (Equation 2.1).

$$K_d = \frac{(C_0 - C_1)}{C_1} * \frac{V}{M * F} \quad (2.1)$$

where C_0 = the initial ion concentration (mmol mL^{-1}) in the experimental solution prior to contact,
 C_1 = the equilibrium ion concentration after contact,
 V = the solution volume (mL),
 M = the exchanger mass (g), and
 F = the mass of dry ion exchanger divided by the mass of wet exchanger (F-factor).

The ion exchange material loading can be calculated from Equation 2.1 by determining the amount of an ion removed from solution divided by the mass of the exchange material and converting to the appropriate units (e.g., mmol g⁻¹) as shown in Equation 2.2.

$$\text{Exchanger loading (mmol g}^{-1}\text{)} = K_d * C_1 \quad (2.2)$$

The column distribution ratio, λ , is obtained by multiplying K_d by the exchanger bed density, ρ_b (g of resin per mL of resin in solution) as shown in Equation 2.3.

$$\lambda = K_d * \rho_b \quad (2.3)$$

The lambda value provides a method of comparing the ion exchange performance of a wide variety of materials on a volume basis. Comparing materials on a volume basis provides an estimate of the ion loading with respect to the column size required. However, the bed density of each material is highly variable depending on solution conditions, column size, and loading methods and has a great effect on the ion loading per material volume. Other methods of comparison (e.g., mass, cost, cycles, effluent composition, waste generation, ease of use) also may be important, but have not been evaluated in this study. Such comparisons may be better suited for engineering trade studies. In particular, use of certain materials in a column may not be possible (e.g., finely powdered solids) and comparison on a mass basis may be more meaningful.

The experimental equipment required to complete the batch K_d determinations included an analytical balance, an oven for F-factor determinations, a variable speed shaker table, 100-mL glass bottles, 0.2- μ m syringe filters, the appropriate ion exchangers, and simulant solutions. Samples were placed into a controlled temperature environment at 25°C and agitated with a "ping-pong" type shaker table at approximately 2 Hz. After reaching the appropriate contact duration (72 hours), the samples were removed from the shaker table and the solids were separated from the liquid by filtration through a 0.2- μ m syringe filter. The filtered solutions were analyzed for ¹³⁷Cs or ⁸⁵Sr by gamma energy analysis (GEA) counting using a NaI crystal. Each 3-mL sample was counted for 20 minutes. Process control blanks were prepared with no sorbent material added and were treated in the same manner as the samples. Analysis of these samples yields the value of C_0 in Equation 1.

In general, the uncertainties associated with the λ and K_d values are estimated to be less than 50%. Calculation of standard deviations (σ) for duplicate samples shows that σ is generally less than 20%. The values of K_d and λ exhibit the greatest uncertainty at very high and very low values. In the former case, as the concentration C_1 in Equation 2.1 begins to approach the detection limit, the analytical uncertainty of the value increases which, in turn, dictates that uncertainty in the K_d value increases. For example, since much of the data collected in this experiment is very close to the analytical detection limit, the error associated with a specific data point is unusually large, often exceeding 100% near the detection limit (e.g., within ten times). A duplicate measurement may differ by nearly an order of magnitude. At the opposite end of the spectrum (e.g., K_d and λ values are low), only small amounts of radionuclide are

removed and the small difference in concentration ($C_0 - C_1$) generates uncertainty levels exceeding 100%. In certain cases, this difference may even yield invalid (negative) K_d values.

2.2 Material Selection and Preparation

Table 2.1 lists the exchangers evaluated in the current experiment, along with selected manufacturing information for each material. Several of these materials are still under development and may or may not be in their optimal form. Some of the materials were specifically designed for cesium (e.g., SuperLig® 644, CS-100, R-F) or strontium removal in the highly caustic or high ionic strength solutions that exist in many of the alkaline wastes in Hanford tanks (Van Vleet 1993) and, therefore, do not perform as well in the neutral pH N-Basin waters. These materials were tested for comparison purposes only and do not necessarily represent the optimum conditions and/or performance of the specific materials.

The potassium cobalt hexacyanoferrate (KCoHex) is an inorganic material produced by 3M (St. Paul, MN) on an experimental basis for incorporation into proprietary web-like membranes (e.g., Empore™ and other materials). The membranes have been used previously for pretreating waste (Bray et al. 1995a; Bray et al. 1995b; Brown 1996a; Brown 1996c; Brown 1996d; Herbst et al. 1995). Two batches (milled and unmilled) were obtained from the New Products Department at 3M and were evaluated in the current experiment.

Professor Abraham Clearfield and coworkers at Texas A&M University have investigated and produced several highly selective inorganic ion exchangers for removing cesium and strontium from various waste matrices. One promising group of materials is the modified natural biotite and phlogophite micas, which are chemically and thermally stable layered aluminosilicate micas in the potassium form. Researchers at Texas A&M and AlliedSignal have developed several methods for converting the natural potassium micas into the sodium forms which, in turn, can more readily exchange for cesium under certain low potassium conditions. In addition, another class of inorganic exchangers with a titanosilicate pharmacosiderite structure has been synthesized and evaluated.

IONSIV® IE-96 is a synthetic high-capacity aluminosilicate zeolite produced by UOP (Des Plaines, IL) with relatively little selectivity for cesium over other alkali metals. TIE-96 is a modified version of the IE-96 and is capable of removing strontium and plutonium, in addition to cesium, from alkaline solutions (Bray et al. 1984; Bray and Hara 1991). Both of these materials have been commercially available for several years. Clinoptilolite is a relatively inexpensive natural zeolite mineral that is capable of removing strontium and, to a lesser degree, cesium from low sodium solutions.

Also produced by UOP are the powdered (IONSIV® IE-910) and engineered (IONSIV® IE-911) forms of the crystalline silicotitanate (CST), respectively. The engineered CST (IONSIV® IE-911) was developed by UOP (Des Plaines, IL) under a Cooperative Research and Development Agreement (CRADA) with Sandia National Laboratory (SNL). The CSTs were originally developed in a powdered form by R. G. Dosch at SNL and Professor R. G. Anthony at Texas A&M. Three batches of engineered

Table 2.1. Selected Physical Properties of Cesium and Strontium Selective Materials

| Material | ID | Batch Number | F-Factor | Date of Manufacture | Particle Size (Mesh) |
|-------------------------|----|--|----------|---------------------|----------------------|
| KCoHex | A | 3M #2999-14 | 0.9655 | April 1996 | unmilled |
| KCoHex | B | 3M #2999-14 | 0.9531 | April 1996 | milled |
| Pharmacosiderite | C | TAMU #TSP-137 | 0.9745 | May 1995 | powder |
| Pharmacosiderite | D | TAMU #E-B Pharm-1 | 0.8641 | May 1995 | powder |
| Pharmacosiderite | E | TAMU #E-B Pharm-2 | 0.6547 | May 1995 | powder |
| Phlogopite 90% Na | F | TAMU #M203 L1-48-12 | 0.8226 | May 1995 | powder |
| Biotite 60% Na | G | TAMU #M178 L1-15-16 | 0.8705 | May 1995 | powder |
| Modified Biotite | H | AS #8212-32A | 0.7781 | May 1995 | powder |
| Modified Biotite | I | AS #8212-15D | 0.8811 | May 1995 | powder |
| Modified Biotite | J | AS #8212-15E | 0.8576 | May 1995 | powder |
| Modified Biotite | K | AS #8212-5-3 | 0.8233 | May 1995 | powder |
| IONSIV® IE-96 | L | UOP #939691090035-C | 0.9653 | June 1992 | 20 - 50 |
| IONSIV® TIE-96 | M | UOP #975791000012-A | 0.8789 | Sept 1995 | 20 - 50 |
| IONSIV® IE-910 | N | UOP #993794040002 | 1.0416 | Sept 1994 | powder |
| IONSIV® IE-911 | O | UOP #07398-38B | 0.9312 | June 1995 | 20 - 50 |
| IONSIV® IE-911 | P | UOP #8671-08 | 0.9621 | June 1995 | 20 - 50 |
| IONSIV® IE-911 | Q | UOP #999096810002 | 0.7383 | Feb 1996 | 20 - 50 |
| SuperLig® 644 | R | 10-SM-171 | 0.8291 | Nov 1994 | 25 - 45 |
| Duolite C-467 | S | Rohm & Haas #6-8189 Lot# L-497107 | 0.4221 | | 50 - 70 |
| Duolite CS-100 | T | Rohm & Haas #6-8144 Lot# L-2-850001 | 0.6148 | Nov 1991 | 20 - 45 |
| Amberlite IRC-76 | U | Rohm & Haas #6-9850 Lot# L-447613 | 0.4964 | | 20 - 45 |
| Amberlite IRC-718 | V | Rohm & Haas #6-2144 Lot# L-2-4902 | 0.5301 | | 20 - 45 |
| Resorcinol-Formaldehyde | W | BSC-187-210 | 0.8522 | Aug 1991 | 40 - 70 |
| Amberlite CG-120 | X | Rohm & Haas #790-170 | 0.8957 | < 1990 | < 200 |
| Clinoptilolite | Y | Natural Zeolite | 1.0675 | Feb 1996 | 20 - 50 |

IE-911 (-999, -08 and -38B) and one batch of the powder were investigated in these experiments. Commercial samples of IE-911 initially became available in January 1996. Numerous experimental studies describing radionuclide uptake under a wide variety of solution conditions are available in the literature (Anthony et al. 1993; Anthony et al. 1994; Bray et al. 1993b; Brown et al. 1996b; Dosch et al. 1993; Klavetter et al. 1994; Marsh et al. 1994; Marsh et al. 1995; Miller and Brown 1997; Svitra et al. 1994; Zheng et al. 1995).

The SuperLig® 644 polymer resin is the latest version of the covalently bound SuperLig® macrocycle family of sequestering ligands from IBC Advanced Technologies (American Fork, UT). It has been shown to be chemically and radiochemically stable and highly selective for cesium even in the presence of excess sodium or potassium (Bray et al. 1995a; Brown et al. 1995a; Brown et al. 1995b; Brown et al. 1995c; Brown et al. 1996a; Brown et al. 1996b; Brown et al. 1996c).

CS-100 and resorcinol-formaldehyde (R-F) are two organic ion exchange resins that are commercially available and under consideration for cesium removal from Hanford tank wastes (Eager et al. 1994; Kurath et al. 1994; Orme 1995; Penwell et al. 1994; Gallagher 1986^(a)). CS-100 is a granular (20 to 50 mesh) phenol-formaldehyde condensate polymer ion exchange resin that is commercially available from Rohm & Haas. R-F, originally developed by J. P. Bibler and R. M. Wallace at WSRC and currently produced by Boulder Scientific (Mead, CO), has been shown to exhibit a much greater loading for cesium and selectivity over sodium or potassium than the CS-100 resin (Bibler et al. 1989; Bibler 1994; Bray et al. 1990; Bray et al. 1992; Bray et al. 1993a; Brown et al. 1995b; Kurath et al. 1994). The chemical and radiation stability (Bibler 1991; Bibler and Crawford 1994; Brown et al. 1995c; Carlson et al. 1995) and the structure/function relationship (Hubler et al. 1995; Hubler et al. 1996a; Hubler et al. 1996b) of the R-F resin to the ion exchange process have been studied extensively.

Duolite C-467, produced by Rohm & Haas, is an organic cation exchanger containing aminophosphonic acid groups on a styrene-divinylbenzene polymer backbone. Amberlite IRC-76 and IRC-718 have a similar polymeric backbone functionalized with chelating aminodiacetate groups. All of these materials are expected to have a greater affinity for strontium than cesium under most conditions. Amberlite CG-120 is a strong acid cation exchanger (sulfonic acid type), again based on the styrene-divinylbenzene polymer. This nonselective exchanger should not pick up cesium or strontium.

Because of different manufacturing processes, each material does not necessarily contain the same counter ion when received from the manufacturer. KCoHex and R-F are in the potassium form while all of the Texas A&M/AlliedSignal micas are specifically converted from the potassium to the sodium forms. CS-100 and SuperLig® 644 are manufactured in the hydrogen form while TIE-96, IE-910, IE-911, and all of the other organic resins are likely in the sodium form. It is possible that, because of variations in the counter ion form of each material, the equilibrium composition of the waste after the exchange process has been completed may vary slightly from exchanger to exchanger. For example, as solution-phase cesium exchanges with K^+ in the R-F resin, the concentration of the K^+ in solution must concurrently increase. As a second example, when cesium exchanges with a proton from the SuperLig® 644 resin, the acidity of the final solution will increase, thereby inducing an additional resistance to further ion exchange.

All materials were used "as received" without additional processing or conversion to a secondary ionic form (e.g., either drying or conversion to the hydrogen or sodium forms). However, the K_d data

(a) Gallagher, S. A. 1986. *Report of Current NCAW Ion Exchange Laboratory Data*. Internal Letter #65453-86-088, Rockwell International, Richland, Washington.

(Section 2.1) obtained during the batch contact are mass corrected (e.g., reported on a dry mass basis) to account for the fraction of easily removed water using the F-factor. Approximately 0.5 g of each material was weighed before and after drying at 105°C for 24 hours. In order to ensure that a constant weight had been achieved, the materials were dried for a second 24-hour period and re-weighed.

2.3 Waste Composition and Preparation

Table 2.2 lists the chemical and radiochemical composition of the actual 105 N-Basin water used in the current experiment. The water sample (#55082-02) was collected in two 10-L plastic containers by Karl Hulse on October 31, 1995, at 10:45 a.m. at N-Basin sample point #2. The sample was graciously supplied to the author by David A. Nelson (PNNL). A small portion of the water was analyzed at the 325 Building Analytical Chemistry Laboratory (ALO #96-2802) for alpha total (AT), GEA, ⁹⁰Sr, total inorganic carbon (TIC), total organic carbon (TOC), ion chromatography (IC), inductively coupled

Table 2.2. Chemical Composition of the 105 N-Basin Water

| Species | Concentration (mol/L) | Concentration (mg/L) |
|-------------------|-----------------------|----------------------|
| Al | 2.892E-05 | 7.80E-01 |
| B | 2.627E-03 | 2.84E+01 |
| Ba | 2.270E-05 | 3.12E+00 |
| Ca | 8.333E-04 | 3.34E+01 |
| Cs | 4.870E-10 | 6.47E-05 |
| K | 6.400E-05 | 2.50E+00 |
| Mg | 2.900E-05 | 7.00E-01 |
| Na | 1.619E-03 | 3.72E+01 |
| Sr | 4.450E-06 | 3.90E-01 |
| CO ₃ | 1.080E-03 | 6.48E+01 |
| Cl | 1.213E-03 | 4.30E+01 |
| F | 6.320E-06 | 1.20E-01 |
| NO ₃ | 8.900E-06 | 5.50E-01 |
| SO ₄ | 1.395E-04 | 1.34E+01 |
| ¹³⁷ Cs | 1.740E-06 | Ci L ⁻¹ |
| ⁹⁰ Sr | 6.130E-06 | Ci L ⁻¹ |
| ¹³⁴ Cs | 1.540E-09 | Ci L ⁻¹ |
| ⁶⁰ Co | 1.200E-09 | Ci L ⁻¹ |
| ¹²⁵ Sb | 4.450E-09 | Ci L ⁻¹ |
| AT | 1.480E-09 | Ci L ⁻¹ |
| pH | 8.30 | pH unit |
| TDS | <2.50E-01 | g L ⁻¹ |

plasma (ICP), pH, total dissolved solids (TDS), and particle size analysis. The majority (82%) of the particle volume consisted of particles with diameters between 10 and 50 microns ($1.0\text{E-}06$ m). The chemical analyses are reported in Table 2.2.

The actual 105 N-Basin water was modified slightly by adding trace levels of ^{85}Sr to facilitate chemical analysis of the strontium concentration and evaluation of the strontium uptake. GEA was used to determine the total cesium and strontium concentrations calculated from the radionuclide content and radioactive isotope fraction. Except for the addition of ^{85}Sr , no further pretreatment (e.g., filtration, precipitation, or chemical addition) of the water was completed. The water was stored in a dark insulated container at room temperature for several weeks prior to actual experimentation. Algae was visible and no attempt was made to destroy or control it.

In addition to the actual 105 N-Basin water, several simulated solutions were prepared that contained the same chemical constituents as the actual water, with the exception of TDS and organic components. Table 2.3 lists the basic composition of the simulant formulation. The total cesium concentration of the basic formulation was varied between $1.00\text{E-}04$ M Cs and $2.6\text{E-}10$ M Cs in order to provide a wide range of cesium concentrations for evaluating ion exchanger performance. In comparison, the actual N-Basin water was estimated to contain approximately $4.87\text{E-}10$ M Cs based on the level of radioactive ^{137}Cs , chemical analysis of the nonradioactive cesium by graphite furnace atomic absorbance spectroscopy (GFAAS), and the estimated ratio of radioactive-to-nonradioactive cesium.

Table 2.3. Chemical Composition of the Simulated 105 N-Basin Water

| Component | Formula Weight (g) | Molarity (mol/L) | Mass Used (g per 30 L) |
|---|--------------------|--------------------|------------------------|
| H_3BO_3 | 61.84 | $2.627\text{E-}03$ | 4.8736 |
| NaF | 41.99 | $6.320\text{E-}06$ | 0.0080 |
| KCl | 74.55 | $6.400\text{E-}05$ | 0.1431 |
| $\text{Ca}(\text{CO}_3)_2$ | 160.10 | $1.850\text{E-}04$ | 0.8886 |
| CaCl_2 | 110.98 | $5.745\text{E-}04$ | 1.9127 |
| $\text{Ca}(\text{OH})_2$ | 74.10 | $7.380\text{E-}05$ | 0.1641 |
| Na_2CO_3 | 105.99 | $7.100\text{E-}04$ | 2.2576 |
| Na_2SO_4 | 142.04 | $9.610\text{E-}05$ | 0.4095 |
| $\text{Ba}(\text{OH})_2 \cdot 8\text{H}_2\text{O}$ | 315.50 | $2.270\text{E-}05$ | 0.2149 |
| $\text{Al}_2(\text{SO}_4)_3 \cdot 18\text{H}_2\text{O}$ | 666.50 | $1.446\text{E-}05$ | 0.2891 |
| $\text{Mg}(\text{OH})_2$ | 58.33 | $2.900\text{E-}05$ | 0.0507 |
| $\text{Sr}(\text{NO}_3)_2$ | 211.63 | $4.450\text{E-}06$ | 0.0283 |
| CsNO_3 | 196.91 | Variable | Variable |

2.4 Simulant Test Conditions

To obtain batch distribution data over a wide range of equilibrium cesium concentrations and to adequately bracket the actual waste composition, a series of batch distribution tests were completed using simulated N-Basin water at the conditions shown in Table 2.4. The simulated solutions were prepared in 5-L batches designated NB4, NB5, NB6, NB7, NB8, and NB9. Each solution was prepared at least 24 hours in advance and was stirred a minimum of 4 hours before being transferred into the individual 100-mL bottles. Approximately 100 mL of solution was transferred into each previously tared bottle and the exact volume of solution was determined by weight and solution density. The bottles also contained the individual ion exchange material preweighed (0.00001 g accuracy) to 0.010 ± 0.001 g. There were a total of 24 exchangers and one control blank in duplicate for a total of 50 separate 100-mL bottles per simulant solution, for a total of 300 solutions.

As described in Section 2.1, each contact involved 100 mL of actual N-Basin water with 0.010 ± 0.001 g of exchanger. The samples were agitated for 72 hours at the ambient temperature of the laboratory (23°C). Following the solid/liquid contact, the solution was separated from the exchanger by filtration through individual 0.2- μ m syringe filters and 3.0-mL aliquots of solution were analyzed for ^{137}Cs and ^{85}Sr by GEA.

2.5 Actual Waste Test Conditions

The batch contacts with the actual 105 N-Basin water were conducted in the same manner as the simulant tests, except the actual water was used in place of the simulant. The actual basin water was designated as "NB0" and was estimated to contain an initial total cesium concentration of $4.87\text{E-}10$ M Cs. As described above and in Section 2.1, each contact involved 100 mL of actual N-Basin water with 0.010 ± 0.001 g of exchanger. The samples were agitated for 72 hours at the ambient temperature of the

Table 2.4. Simulant Testing Conditions

| Experimental Parameter | Experimental Conditions |
|--------------------------|--|
| Exchangers | Twenty-four individual materials |
| Waste solution | 105 N-Basin water simulant |
| Initial Na concentration | $1.62\text{E-}03$ M Na |
| Initial Cs concentration | $1.0\text{E-}04$, $1.0\text{E-}05$, $1.0\text{E-}06$, $1.0\text{E-}07$, $1.0\text{E-}08$, and $2.6\text{E-}10$ M Cs |
| Waste volume | 100 mL |
| Exchanger mass | 0.010 ± 0.001 g |
| Contact time/temperature | 72 hr, 23°C |
| Tracers | ^{137}Cs , ^{85}Sr |

laboratory (23°C). Following the solid/liquid contact, the solution was separated from the exchanger by filtration through individual 0.2- μm syringe filters and 3.0-mL aliquots of solution were analyzed for ^{137}Cs and ^{85}Sr by GEA.

3.0 Results and Discussion

Twenty-four organic and inorganic ion exchange materials were evaluated for their performance in cesium and strontium uptake from actual and simulated basin water at the 100 Area N-Reactor. Cesium and strontium batch distribution coefficients (K_d s), material loadings (mmol g^{-1}), decontamination factors (DF), and percent removal (%R) were determined for each material and are presented here. The appendix provides a complete listing of these data.

3.1 Simulated N-Basin Water Results

3.1.1 Cesium Batch Distribution

The cesium K_d values in several simulated N-Basin waters are displayed in Figure 3.1 as a function of equilibrium cesium concentration for every ion exchange material evaluated. The plot displays the results for all of the exchangers on a single logarithmic graph that provides a broad view of the entire data set. Although the data are much too cluttered to allow simple visualization of the performance of a single exchanger, they clearly illustrate a distinct delineation between each solution (NB4, NB5, NB6, NB7, NB8, and NB9). All of the data for a particular solution (i.e., different cesium concentration) fall on a slightly bent curve as plotted in the log-log format, irrespective of ion exchange material.

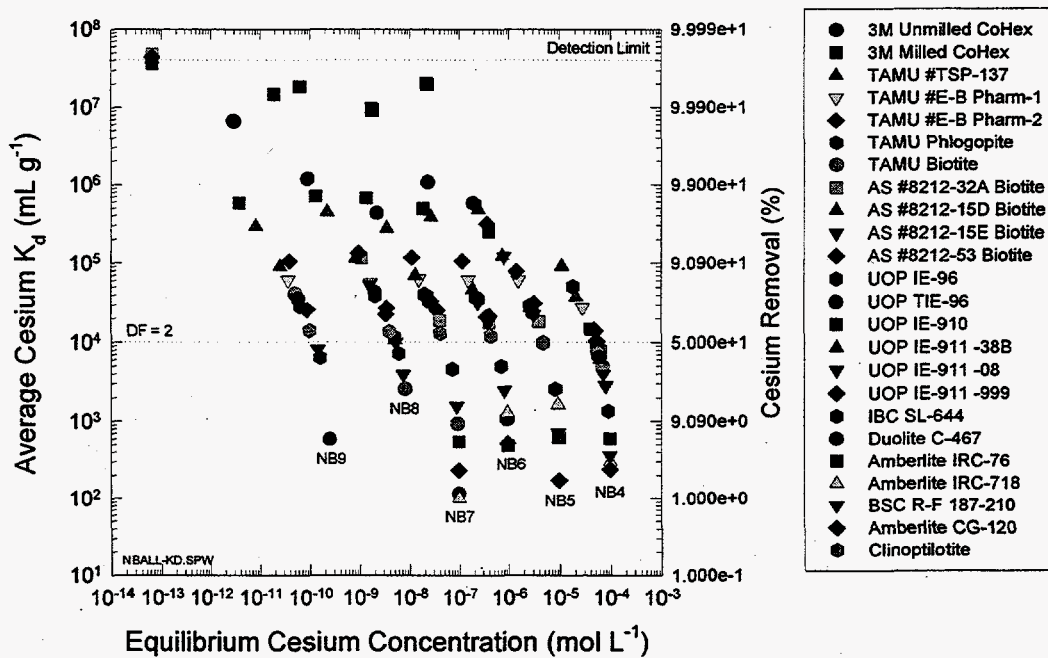


Figure 3.1. Average Batch Distribution Coefficients for Cesium as a Function of Equilibrium Cesium Concentration for 24 Ion Exchange Materials in Simulated 105 N-Basin Water

The materials which exhibit low K_d values (e.g., those below the liquid:solid phase ratio, about $1.00E+04 \text{ mL g}^{-1}$) do not remove cesium to any appreciable extent and therefore cluster around the initial cesium concentration of the solution. On the graph, the data points lay on a vertical line where K_d increases from $1.00E+01$ to $3.00E+03 \text{ mL g}^{-1}$ while the cesium concentration remains relatively constant (e.g., $1.00E-04 \text{ M Cs}$ for solution NB4, $1.00E-05 \text{ M Cs}$ for solution NB5, etc.). At or near a cesium K_d value of $1.0E+04 \text{ mL g}^{-1}$, 50% of the cesium is removed. The inflection point occurs at a K_d value equal to the solution-to-mass phase ratio (V/M). Beyond this point, every tenfold increase in the K_d value is associated with a tenfold decrease in equilibrium cesium concentration. This phenomena is a result of the mathematical nature of the K_d equation (Equation 2.1) and occurs with all of the N-Basin solutions, irrespective of the initial cesium concentration.

The materials that exhibited the lowest cesium K_d values (e.g., those below $1.00E+04 \text{ mL g}^{-1}$) included Amberlite IRC-718, Amberlite CG-120, Amberlite IRC-76, Duolite C-467, the R-F resin BSC-187-210, SuperLig® 644, and natural clinoptilolite in increasing order of K_d . The Amberlite and Duolite resins are strong acid-type cation exchangers and are not expected to be capable of selectively removing cesium from solution. Natural clinoptilolite, with K_d values just slightly above the liquid:solid phase ratio (ca. $1.30E+04 \text{ mL g}^{-1}$), is a high-capacity inorganic zeolite with a relatively low selectivity for cesium and strontium. These materials were included in the current test to evaluate the hypothesis that a nonselective cation exchange resin or natural mineral could be used to efficiently remove cesium from a low ionic strength solution with minimal ionic interferences. The data do not support this theory and it is apparent that high selectivity is necessary even in these low ionic strength matrices. The relatively low K_d results for the SuperLig® 644 and R-F resins are as expected since these materials are known to load cesium in highly caustic solution and elute cesium in acidic and neutral pH solutions.

As is shown in Figure 3.1, most of the ion exchange materials evaluated demonstrated average performance, with cesium K_d values between $1.00E+05$ and $1.00E+06 \text{ mL g}^{-1}$ over the range of cesium concentration from $1.0E-05$ to $1.0E-10 \text{ M}$ at equilibrium. These values correspond to a removal of between 50% and 91%. Although the data are somewhat varied, exchangers of this group include most of the inorganic materials from AlliedSignal, Texas A&M, and UOP. Two of the IE-911 exchangers exhibit K_d values of $1.0E+05 \text{ mL g}^{-1}$.

Those materials that performed exceptionally well include, in increasing order of K_d , the Texas A&M TSP-137, the UOP IE-910 powder, and the unmilled and the milled KCoHex from 3M. The data for the powdered IE-910 and the milled KCoHex, when compared to the larger particle IE-911 or unmilled KCoHex, suggest the contact time to reach equilibrium may not have been sufficient. Evidently either some ion exchange sites are obstructed or the exchange kinetics are slower in the larger particle materials. Several materials (AlliedSignal biotite #8212-32A, #8212-53, and Texas A&M phlogopite) exhibited scattered K_d values ranging from $1.0E+04$ to $5.0E+07 \text{ mL g}^{-1}$ (the detection limit), depending upon the cesium concentration. As was mentioned in the experimental section, the error associated with these high K_d values is substantial and duplicate measurements were widely scattered.

The cesium K_d results for five selected materials are displayed in Figure 3.2 as a function of equilibrium cesium concentration in simulated N-Basin water. This is a subset of the results displayed in Figure 3.1 and represents a range of data which are readily visible on the graph. The data profile is similar to that observed previously for cesium removal by ion exchange batch distribution tests from simulated and actual tank wastes (Bray et al. 1992; Bray et al. 1993a; Brown et al. 1995c; Brown et al. 1996b; Kurath et al. 1994). In general, for every material, the cesium K_d is nearly constant at low cesium concentration (e.g., less than $1.0E-06$ M Cs) but decreases at higher concentration (e.g., greater than $1.0E-05$ M Cs). For example, in the simulated water, clinoptilolite exhibits a cesium K_d of approximately $1.3E+04$ mL g^{-1} between $1.0E-10$ and $1.0E-06$ M Cs. Between $1.0E-04$ and $1.0E-05$ M Cs, the cesium K_d decreases to $7.0E+03$ mL g^{-1} . The data exhibit a smooth curvature over the entire cesium concentration range in the simulated solutions. Similar profiles have been noted previously for zeolite-type exchangers. In contrast, the higher performance materials (e.g., KCoHex and IE-910) display significantly larger cesium K_d values (e.g., $2.0E+07$ and $6.0E+05$ mL g^{-1} , respectively) at lower equilibrium concentration. However, at cesium levels near $1.0E-04$ M, the K_d values deteriorate dramatically to the same levels as with the clinoptilolite material (e.g., $1.3E+04$ and $7.0E+03$ mL g^{-1} , respectively). The data indicate that, to some extent, the performance of each material may improve as the cesium concentration in solution is reduced. However, at extremely low levels, the performance of all materials is independent of cesium concentration.

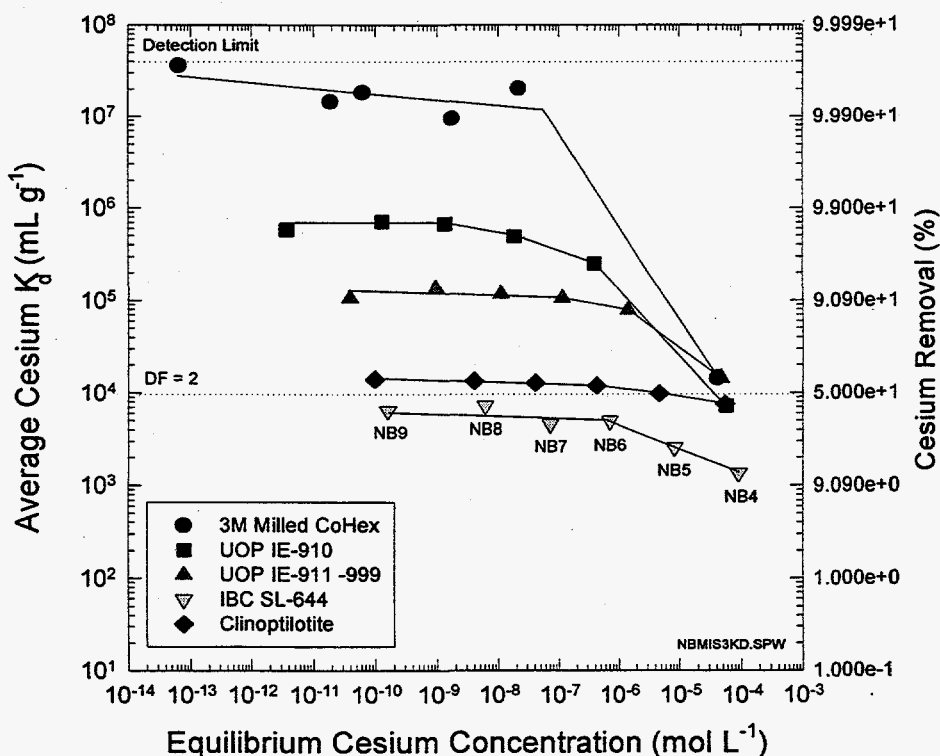


Figure 3.2. Average Batch Distribution Coefficients for Cesium as a Function of Equilibrium Cesium Concentration for Selected Ion Exchange Materials in Simulated 105 N-Basin Water

3.1.2 Cesium Loading

Figures 3.3 through 3.5 display the amount of cesium loaded (mmol g^{-1}) on each individual ion exchange material as a function of equilibrium cesium concentration in simulated N-Basin water. Figure 3.3 displays the results for all of the exchangers on a single logarithmic graph that provides a broad view of the entire data set. Although the data are much too cluttered to allow visualization of the performance of a single exchanger, they clearly distinguish between each of the simulant solutions (NB4, NB5, NB6, NB7, and NB9).

All of the data for a particular solution (irrespective of ion exchange material) fall on a bent curve that resembles "boomerang" as plotted in the log-log format. The materials which exhibit low K_d values also exhibit low material loadings and do not remove cesium from solution to any appreciable extent. Therefore, these results cluster around the initial cesium concentration of the solution. For example, for solution NB4, the data points lay on a vertical line where the cesium loading increases by an order of magnitude (e.g., from $2.00\text{E-}02$ to $2.00\text{E-}01 \text{ mmol g}^{-1}$) while the cesium concentration stays relatively constant (e.g., $1.00\text{E-}04 \text{ M Cs}$).

In contrast, at very low cesium levels for a particular solution, the material cesium loading appears to saturate and reach a maximum value. For example, the maximum exchanger loading in solution NB4 is approximately $1.00\text{E+}00 \text{ mmol g}^{-1}$. Each incremental decrease in the equilibrium cesium concentration in solution does not necessarily produce an incremental increase in exchanger loading. The material loading is

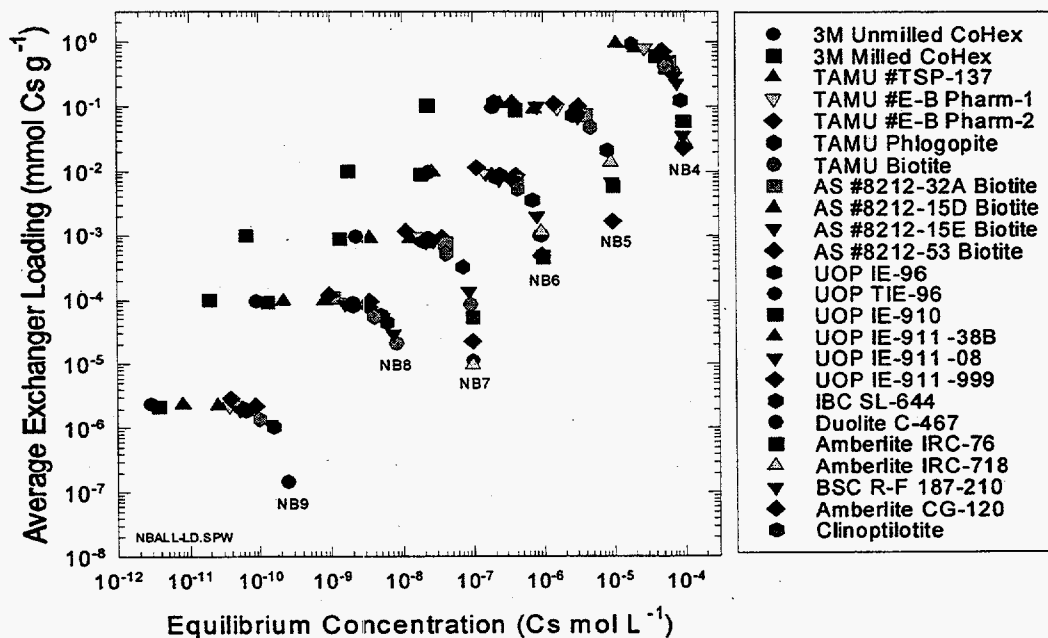


Figure 3.3. Average Cesium Loading as a Function of Equilibrium Cesium Concentration for 24 Ion Exchange Materials in Simulated 105 N-Basin Water

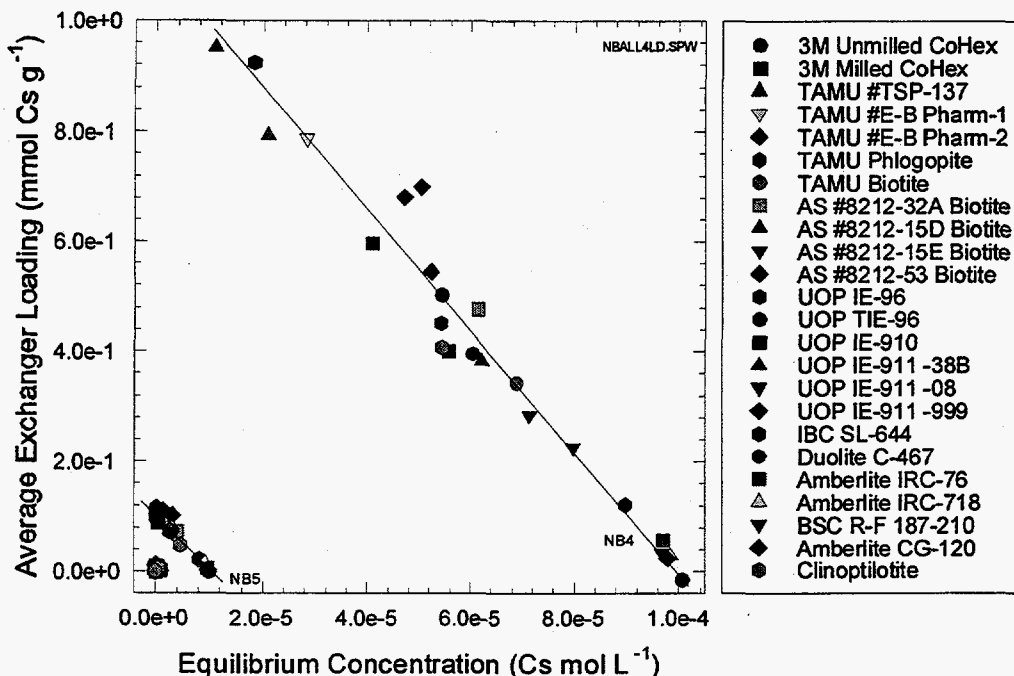


Figure 3.4. Average Cesium Loading as a Function of Equilibrium Cesium Concentration for 24 Ion Exchange Materials in Simulated 105 N-Basin Water

controlled by the amount of cesium removed from solution and can never exceed the amount initially in solution. Although the K_d value may increase dramatically when the percent cesium removal increases from 99.9% to 99.99%, the amount of cesium loaded on the ion exchange material is essentially the same. This phenomena is a result of the mathematical nature of the loading calculation and occurs for all of the N-Basin solutions, irrespective of the initial cesium concentration.

Displaying the same data on a normal linear scale instead of a logarithmic scale produces another interesting visual display as is shown in Figure 3.4. The figure displays the material loading as a function of equilibrium cesium concentration between zero and $1.00E-04$ M Cs. The material loading for a single solution (e.g., NB4) exhibits an inverse linear correlation as a function of the equilibrium cesium concentration. As one might expect, those materials that leave less residual cesium in solution display greater cesium loadings per mass of exchanger. For the highest cesium-containing solution (e.g., NB4 contains $1.00E-04$ M), the maximum cesium loading value approaches 1 mmol g^{-1} for some of the experimental materials from AlliedSignal and Texas A&M. When the loading data for the NB4 solution is extrapolated back to an equilibrium cesium concentration of zero (e.g., complete removal of the cesium initially in solution), the maximum loading for any material is estimated to be approximately 1.15 mmol g^{-1} .

Also evident in Figure 3.4 is the reduced cesium loadings displayed by all exchangers when the initial cesium concentration in solution is decreased by one or more orders of magnitude (e.g., NB5, NB6, etc.).

These data are displayed in a compressed manner next to the origin of both axes and cannot be adequately resolved at this scale. However, when viewed in this way, the data indicate that a tenfold decrease in the initial cesium concentration results in a tenfold decrease in cesium loading

The visual appearance of the loading data versus equilibrium cesium concentration in simulated N-Basin water is substantially different for a small subset of exchangers (Figure 3.5) than for the entire set of materials as is displayed in Figure 3.3. This data subset represents an assortment of exchangers that are readily discernible on the graph. As described in the experimental section, the loading data are calculated from the same experiment as the batch K_d data. While the cesium K_d (Figure 3.2) is nearly constant at low cesium concentration (e.g., less than 1.0×10^{-6} M Cs), the cesium loading is not constant but rather decreases with decreasing equilibrium cesium concentration. The data exhibit a smooth curvature over the entire cesium concentration range in the simulated solutions and indicate that the material performance (e.g., loading) increases as the cesium concentration in solution increases. The total amount of cesium that can be loaded on any exchanger will decrease as the concentration of cesium in solution decreases. This is the intrinsic nature of the ion exchange process and these results have important implications for the remediation of low cesium solutions. Extrapolation of material loading performance at low solution concentrations from higher contaminant levels may be possible with adequate characterization of the process analytical data.

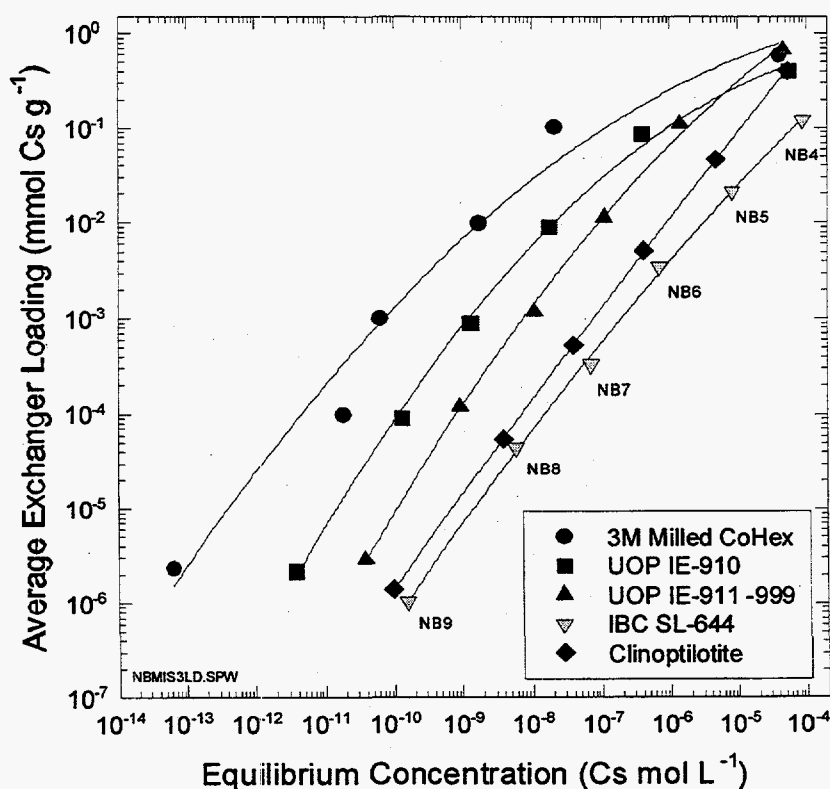


Figure 3.5. Average Cesium Loading as a Function of Equilibrium Cesium Concentration for Selected Ion Exchange Materials in Simulated 105 N-Basin Water

3.1.3 Strontium Batch Distribution

Strontium K_d , loading, DF, and percent removal data were collected for each exchanger in each solution despite the fact that the initial strontium concentration in the simulants was not varied. For this reason, the strontium data for all of the simulant solutions (e.g., NB4, NB5, NB6, NB7, NB8, and NB9) overlay each other. Figure 3.6 displays average K_d data as a function of equilibrium strontium concentration in simulated N-Basin water for all 24 ion exchange materials. In this plot, the results for all of the exchangers are displayed on a single logarithmic graph that provides a broad view of the entire data set. The data are much too cluttered to allow visualization of the performance of a single exchanger or particular solution. However, suppressed Sr K_d values (see Appendix) are observed for the highest cesium-containing solution (NB4), suggesting that two ions may not act independently of each other. The cesium concentration in the NB4 solution is five to six orders of magnitude greater than exists in the N-Basin water and is even one to two orders of magnitude greater than exists in most of the high-level tank waste. Such levels are much greater than would be expected for most ion exchange processes. At lower cesium concentrations (e.g., NB5, NB6, etc.), the cesium level does not appear to influence the Sr K_d values. At these levels the ions do not appear to interact and they may even use different exchange sites or exchange mechanisms.

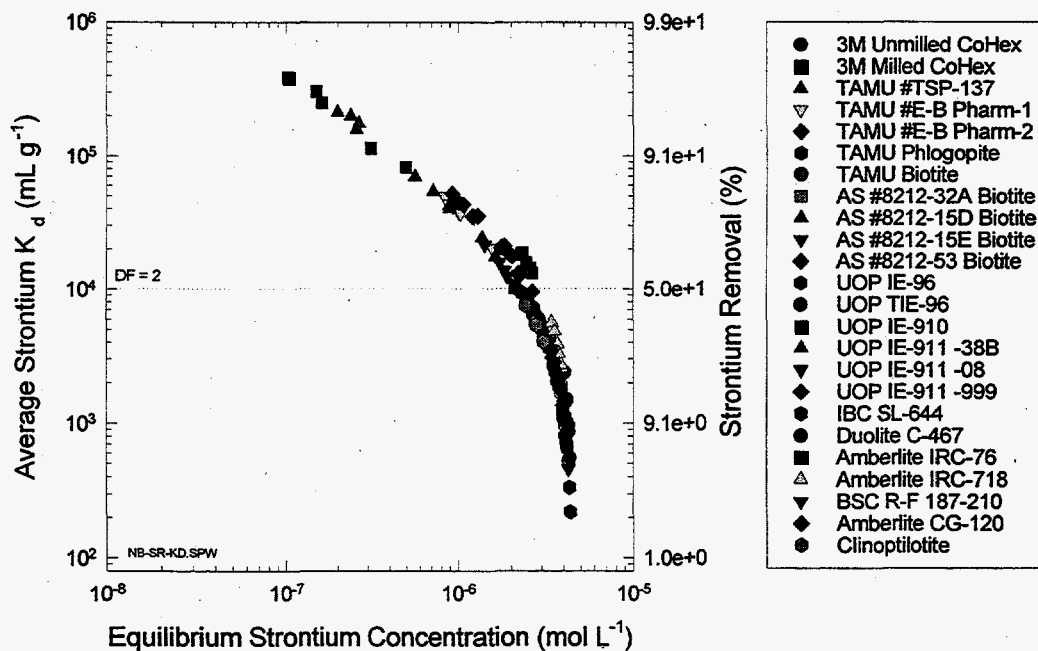


Figure 3.6. Average Batch Distribution Coefficients for Strontium as a Function of Equilibrium Strontium Concentration for 24 Ion Exchange Materials in Simulated 105 N-Basin Water

3.1.4 Strontium Loading

Figure 3.7 displays strontium loading (mmol g^{-1}) on each individual ion exchange material as a function of equilibrium strontium concentration in simulated N-Basin water. In this figure, the results for all of the exchangers are displayed on a single logarithmic graph that provides a broad view of the entire data set. Again, the data are much too cluttered to allow visualization of the performance of a single exchanger, and their appearance is similar to that for the cesium loading results described in Figure 3.3. However, as with the strontium K_d results, the data in the Appendix suggest the material strontium loading is suppressed at the highest cesium concentration (e.g., NB4). Even with this slight correlation with cesium concentration, the data still fall on a bent curve that resembles "boomerang" in the log-log format.

It is interesting to note that two of the exchangers have a dramatically better capability to remove more strontium than can the other materials. The Texas A&M TSP-137 and the UOP IONSIV™ IE-910 reduce the strontium concentration to nearly $1.0\text{E-}07 \text{ M Sr}$, while most of the other materials cannot achieve $1.0\text{E-}06 \text{ M Sr}$. Another observation is the relatively high strontium loading for the Amberlite IRC-76 even though it removes very little strontium from solution. Evidently this results from the low material density. It is likely that adding more exchanger mass would increase the overall percent removal (decontamination factor) and decrease the equilibrium strontium concentration.

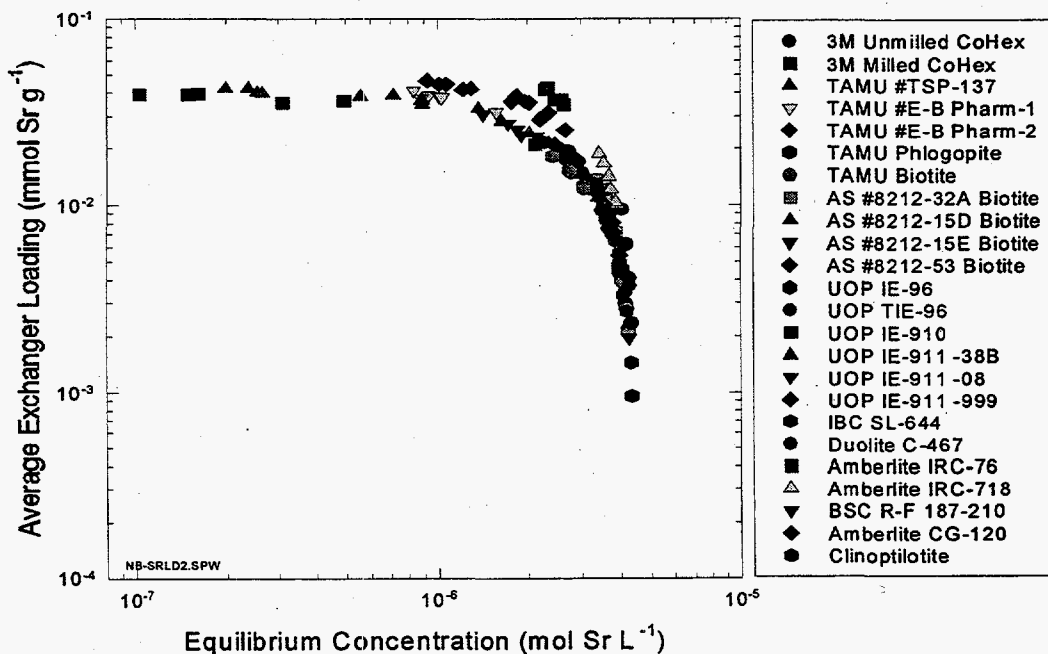


Figure 3.7. Average Strontium Loading as a Function of Equilibrium Strontium Concentration for 24 Ion Exchange Materials in Simulated 105 N-Basin Water

It is also interesting to compare the magnitude of exchanger loading as displayed in Figure 3.7 (strontium loading) and Figure 3.3 (cesium loading). Since the initial strontium concentration in this experiment was $4.45\text{E-}06\text{ M}$, the strontium loading results should lie between solutions NB5 and NB6 as displayed in Figure 3.3. Extrapolation of the cesium data suggests that a maximum cesium loading of approximately $4.0\text{E-}02\text{ mmol g}^{-1}$ should be observed at $4.45\text{E-}06\text{ M}$. This is exactly what is observed for the strontium data, providing further evidence that the material loading is dependent on the equilibrium ion concentration (either cesium or strontium) and not the identity of the ion.

Figure 3.8 displays the same data on a linear scale instead of a logarithmic scale. This figure illustrates the material loading as a function of equilibrium strontium concentration between zero and $5.00\text{E-}06\text{ M Sr}$. The material loading exhibits a linear correlation as was observed for the cesium loading, increasing with decreasing concentration. The material density does appear to affect the amount of strontium loaded on an exchanger. The two lower density exchangers (IRC-76 and IRC-718) have greater slopes, suggesting a greater strontium capacity per unit mass. However, the inorganic TSP-137 and IE-910 appear to be capable of achieving lower equilibrium strontium levels.

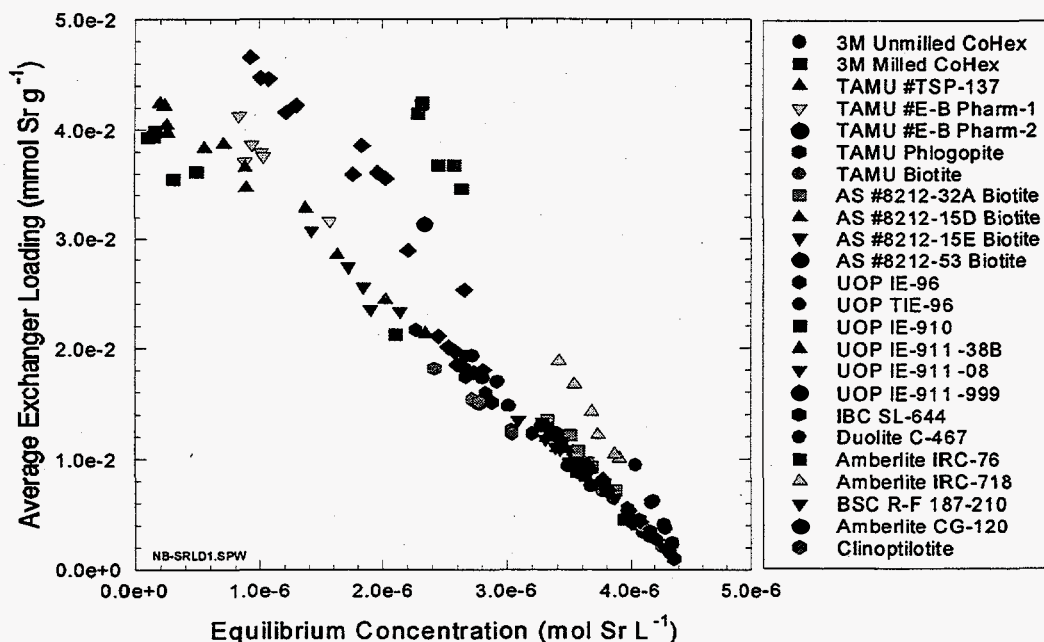


Figure 3.8. Average Strontium Loading as a Function of Equilibrium Strontium Concentration for 24 Ion Exchange Materials in Simulated 105 N-Basin Water

3.1.5 Cesium Dependence on Strontium Results

Figures 3.9 and 3.10 display the effect of the equilibrium cesium concentration on the strontium batch distribution results for the strontium K_d (mL g^{-1}) and loading (mmol g^{-1}), respectively. Only selected exchangers were chosen to illustrate the general appearance of the data set. In addition, only a small subset of the data was connected with lines to avoid cluttering the figure. Certain materials exhibit a greater dependence from the strontium K_d or loading on cesium concentration, but the general trend is readily observed. The strontium K_d or loading is inversely correlated to the cesium concentration (increases with decreasing concentration from $1.0\text{E-}04$ to $1.0\text{E-}09$ M Cs). The data suggest that either the two ions are competing for similar ion exchange sites or the higher cesium loading perturbs the strontium sites and hinders the strontium exchange process.

3.2 Actual Waste Results

3.2.1 Cesium Batch Distribution

Table 3.1 compiles the average cesium batch distribution results (e.g., K_d , DF, loading, and percent removal) for each ion exchange material evaluated in actual N-Basin water. The highest average K_d values for cesium varied from $1.2\text{E}+05$ mL g^{-1} down to approximately $3.0\text{E}+04$ mL g^{-1} . This range corresponds to between 75% and 91% cesium removal. Most of the exchanger results clustered around an average K_d value of $2.0\text{E}+04$ mL g^{-1} . One of the modified biotite micas (#8212-32A) produced by AlliedSignal yielded

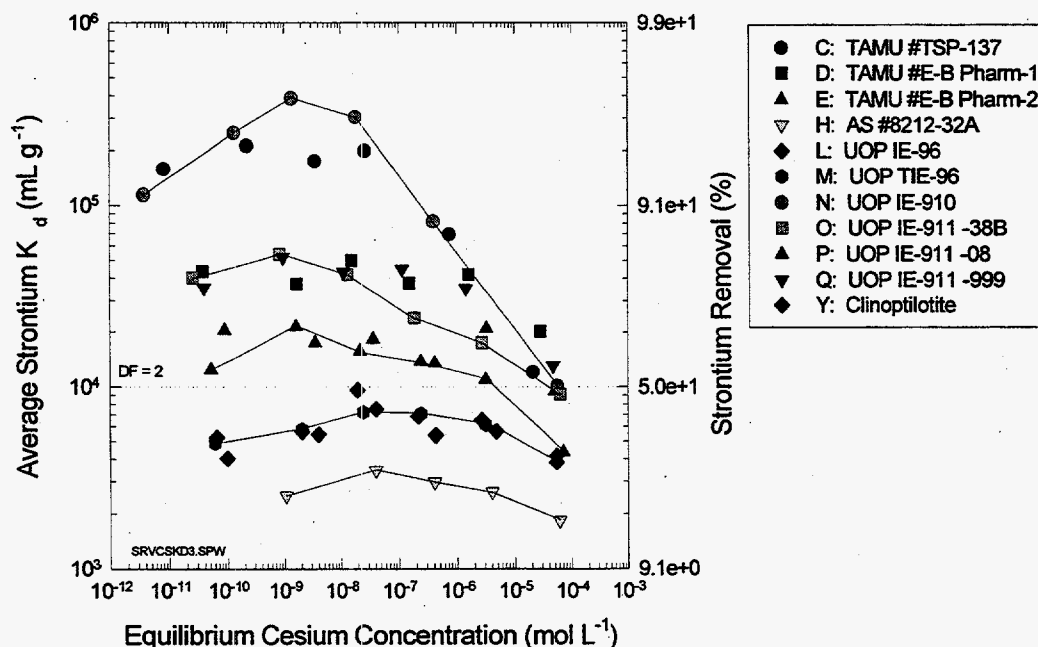


Figure 3.9. Average Batch Distribution Coefficients for Strontium as a Function of the Equilibrium Cesium Concentration for Selected Ion Exchange Materials in Simulated 105 N-Basin Water

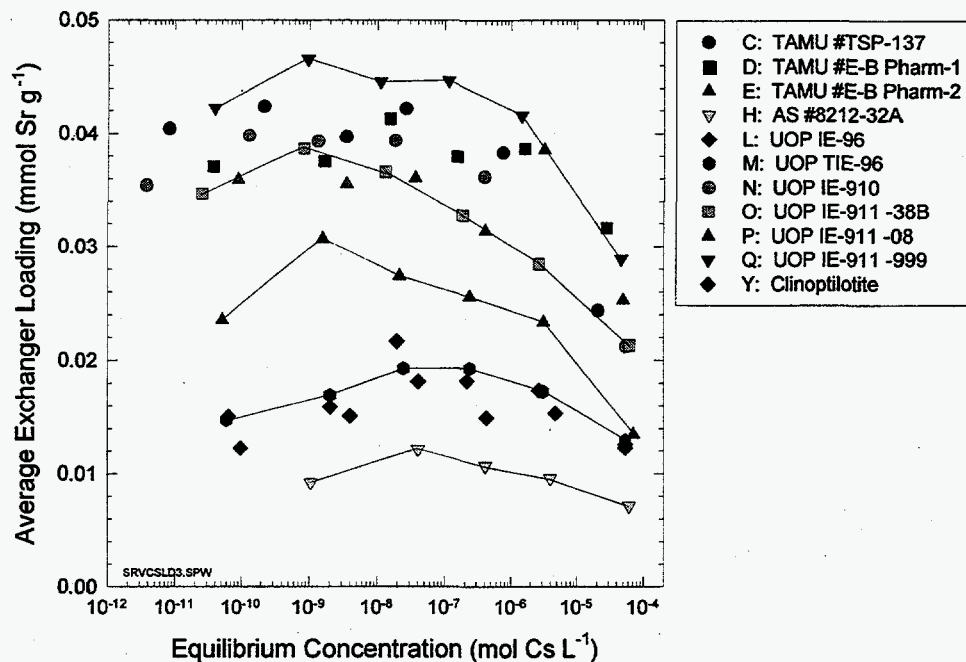


Figure 3.10. Average Strontium Loading as a Function of Equilibrium Cesium Concentration for Selected Ion Exchange Materials in Simulated 105 N-Basin Water

the highest cesium K_d values in the actual N-Basin water. Other materials that produced above-average K_d values included the milled and unmilled KCoHex produced by 3M, other AlliedSignal modified biotites, IE-910 and IE-911 produced by UOP, and a sodium-form phlogopite mica produced by Texas A&M.

As listed in Table 3.1, the lowest average K_d values for cesium varied from $7.6E+03 \text{ mL g}^{-1}$ for natural clinoptilolite down to a negative $2.8E+02 \text{ mL g}^{-1}$ for Amberlite IRC-718. These results correspond to cesium removal from essentially zero to about 45%. These average values are clearly inferior to those described above and these materials should not be used under these conditions. Resorcinol-formaldehyde and SuperLig® 644 gave average K_d values of $5.8E+03$ and $4.6E+03 \text{ mL g}^{-1}$, respectively. Both of these materials are known to remove cesium from highly caustic solutions and only minimally from neutral pH matrices.

3.2.2 Strontium Batch Distribution

Table 3.2 compiles the average strontium batch distribution results (e.g., K_d , DF, loading, and percent removal) for each ion exchange material evaluated in actual N-Basin water. The highest average K_d values for strontium varied from $3.2E+04 \text{ mL g}^{-1}$ down to $7.0E+03 \text{ mL g}^{-1}$. TSP-137, produced by Texas A&M, yielded the highest K_d values for strontium in the actual N-Basin water, followed by IE-910 and IE-911 produced by UOP, two pharmacosiderites produced by Texas A&M, and Amberlite IRC-76 produced by Rohm & Haas. These values correspond to strontium removal in the range of 60% to 80%.

Table 3.1. Summary of Averaged Cesium Batch Distribution Results from Actual 105 N-Basin Water

| Material | ID | Batch Number | [Cs] Final (mol L ⁻¹) | Cs K _d (mL g ⁻¹) | Cs DF (C ₀ /C _i) | Cs Load (mmol g ⁻¹) | Percent Cs Removal |
|-------------------------|----|--|--------------------------------------|--|--|------------------------------------|-----------------------|
| KCoHex | A | 3M #2999-14 | 4.869E-11 | 8.781E+04 | 1.001E+01 | 4.271E-06 | 90.002% |
| KCoHex | B | 3M #2999-14 | 4.355E-11 | 1.022E+05 | 1.121E+01 | 4.435E-06 | 91.057% |
| Pharmacosiderite | C | TAMU #TSP-137 | 1.357E-10 | 2.466E+04 | 3.599E+00 | 3.335E-06 | 72.126% |
| Pharmacosiderite | D | TAMU #E-B Pharm-1 | 1.177E-10 | 4.079E+04 | 4.677E+00 | 4.102E-06 | 75.841% |
| Pharmacosiderite | E | TAMU #E-B Pharm-2 | 1.944E-10 | 2.293E+04 | 2.507E+00 | 4.450E-06 | 60.076% |
| Phlogopite 90% Na | F | TAMU #M203 L1-48-12 | 7.865E-11 | 6.051E+04 | 6.192E+00 | 4.759E-06 | 83.849% |
| Biotite 60% Na | G | TAMU #M178 L1-15-16 | 1.481E-10 | 2.486E+04 | 3.296E+00 | 3.667E-06 | 69.598% |
| Modified Biotite | H | AS #8212-32A | 4.438E-11 | 1.235E+05 | 1.097E+01 | 5.483E-06 | 90.887% |
| Modified Biotite | I | AS #8212-15D | 5.576E-11 | 8.540E+04 | 8.738E+00 | 4.760E-06 | 88.551% |
| Modified Biotite | J | AS #8212-15E | 5.956E-11 | 7.990E+04 | 8.194E+00 | 4.745E-06 | 87.769% |
| Modified Biotite | K | AS #8212-5-3 | 7.926E-11 | 6.133E+04 | 6.234E+00 | 4.773E-06 | 83.725% |
| IONSIV® IE-96 | L | UOP #939691090035-C | 1.359E-10 | 2.631E+04 | 3.642E+00 | 3.489E-06 | 72.104% |
| IONSIV® TIE-96 | M | UOP #975791000012-A | 1.772E-10 | 1.868E+04 | 2.748E+00 | 3.311E-06 | 63.604% |
| IONSIV® IE-910 | N | UOP #993794040002 | 4.887E-11 | 8.183E+04 | 9.965E+00 | 3.998E-06 | 89.964% |
| IONSIV® IE-911 | O | UOP #07398-38B | 1.461E-10 | 2.379E+04 | 3.336E+00 | 3.473E-06 | 70.009% |
| IONSIV® IE-911 | P | UOP #8671-08 | 1.923E-10 | 1.525E+04 | 2.541E+00 | 2.922E-06 | 60.514% |
| IONSIV® IE-911 | Q | UOP #999096810002 | 9.668E-11 | 5.362E+04 | 5.046E+00 | 5.170E-06 | 80.148% |
| SuperLig® 644 | R | 10-SM-171 | 3.475E-10 | 4.581E+03 | 1.401E+00 | 1.592E-06 | 28.638% |
| Duolite C-467 | S | Rohm & Haas #6-8189 Lot# L-497107 | 4.688E-10 | 8.840E+02 | 1.039E+00 | 4.083E-07 | 3.730% |
| Duolite CS-100 | T | Rohm & Haas #6-8144 Lot# L-2-850001 | NA | NA | NA | NA | NA |
| Amberlite IRC-76 | U | Rohm & Haas #6-9850 Lot# L-447613 | 4.671E-10 | 8.258E+02 | 1.043E+00 | 3.842E-07 | 4.093% |
| Amberlite IRC-718 | V | Rohm & Haas #6-2144 Lot# L-2-4902 | 4.946E-10 | -2.807E+02 | 9.847E-01 | -1.388E-07 | -1.557% |
| Resorcinol-Formaldehyde | W | BSC-187-210 | 3.202E-10 | 5.779E+03 | 1.523E+00 | 1.844E-06 | 34.258% |
| Amberlite CG-120 | X | Rohm & Haas #790-170 | 4.649E-10 | 5.051E+02 | 1.047E+00 | 2.348E-07 | 4.529% |
| Clinoptilolite | Y | Natural Zeolite | 2.672E-10 | 7.576E+03 | 1.823E+00 | 2.023E-06 | 45.134% |

Most of the ion exchangers exhibited average K_d values for strontium between 1.0E+03 and 5.0E+03 mL g⁻¹. These materials included the phlogopite and biotites produced by Texas A&M and AlliedSignal; IE-96 and TIE-96 produced by UOP; Duolite C-467, Amberlite IRC-718, and Amberlite CG-120 produced by Rohm & Haas; resorcinol-formaldehyde produced by Boulder Scientific; and natural clinoptilolite. The average strontium removal was between 10% and 30%.

The lowest average K_d values for strontium ranged from 1.7E+02 mL g⁻¹ for the SuperLig® 644 and 9.9E+02 mL g⁻¹ for the KCoHex. These values correspond to strontium removal of less than 10%. These values are clearly inferior to those described above and these materials should not be used under these conditions. In fact, most of these materials are extremely selective for cesium and therefore should not be expected to yield large K_d values for strontium.

Table 3.2. Summary of Averaged Strontium Batch Distribution Results from Actual 105 N-Basin Water

| Material | ID | Batch Number | [Sr] Final (mol L ⁻¹) | Sr K _d (mL g ⁻¹) | Sr DF (C ₀ /C _i) | Sr Load (mmol g ⁻¹) | Percent Sr Removal |
|-------------------------|----|--|--------------------------------------|--|--|------------------------------------|-----------------------|
| KCoHex | A | 3M #2999-14 | 4.084E-06 | 8.745E+02 | 1.090E+00 | 3.567E-03 | 8.230% |
| KCoHex | B | 3M #2999-14 | 4.049E-06 | 9.947E+02 | 1.099E+00 | 4.020E-03 | 9.012% |
| Pharmacosiderite | C | TAMU #TSP-137 | 1.006E-06 | 3.258E+04 | 4.433E+00 | 3.271E-02 | 77.404% |
| Pharmacosiderite | D | TAMU #E-B Pharm-1 | 1.977E-06 | 1.527E+04 | 2.376E+00 | 2.746E-02 | 55.575% |
| Pharmacosiderite | E | TAMU #E-B Pharm-2 | 2.608E-06 | 1.075E+04 | 1.708E+00 | 2.802E-02 | 41.401% |
| Phlogopite 90% Na | F | TAMU #M203 L1-48-12 | 3.939E-06 | 1.507E+03 | 1.130E+00 | 5.959E-03 | 11.490% |
| Biotite 60% Na | G | TAMU #M178 L1-15-16 | 3.926E-06 | 1.451E+03 | 1.135E+00 | 5.648E-03 | 11.770% |
| Modified Biotite | H | AS #8212-32A | 3.807E-06 | 2.092E+03 | 1.169E+00 | 7.961E-03 | 14.440% |
| Modified Biotite | I | AS #8212-15D | 3.910E-06 | 1.529E+03 | 1.139E+00 | 5.951E-03 | 12.124% |
| Modified Biotite | J | AS #8212-15E | 3.901E-06 | 1.565E+03 | 1.141E+00 | 6.084E-03 | 12.330% |
| Modified Biotite | K | AS #8212-5-3 | 4.227E-06 | 6.183E+02 | 1.053E+00 | 2.613E-03 | 5.015% |
| IONSIV® IE-96 | L | UOP #939691090035-C | 3.410E-06 | 3.031E+03 | 1.305E+00 | 1.033E-02 | 23.378% |
| IONSIV® TIE-96 | M | UOP #975791000012-A | 3.433E-06 | 3.176E+03 | 1.296E+00 | 1.089E-02 | 22.847% |
| IONSIV® IE-910 | N | UOP #993794040002 | 1.355E-06 | 2.084E+04 | 3.283E+00 | 2.824E-02 | 69.543% |
| IONSIV® IE-911 | O | UOP #07398-38B | 2.117E-06 | 1.123E+04 | 2.103E+00 | 2.377E-02 | 52.434% |
| IONSIV® IE-911 | P | UOP #8671-08 | 2.661E-06 | 6.674E+03 | 1.674E+00 | 1.773E-02 | 40.192% |
| IONSIV® IE-911 | Q | UOP #999096810002 | 1.863E-06 | 1.841E+04 | 2.390E+00 | 3.427E-02 | 58.136% |
| SuperLig® 644 | R | 10-SM-171 | 4.384E-06 | 1.731E+02 | 1.015E+00 | 7.586E-04 | 1.490% |
| Duolite C-467 | S | Rohm & Haas #6-8189 Lot# L-497107 | 4.208E-06 | 1.276E+03 | 1.057E+00 | 5.370E-03 | 5.428% |
| Duolite CS-100 | T | Rohm & Haas #6-8144 Lot# L-2-850001 | NA | NA | NA | NA | NA |
| Amberlite IRC-76 | U | Rohm & Haas #6-9850 Lot# L-447613 | 3.269E-06 | 6.923E+03 | 1.362E+00 | 2.257E-02 | 26.534% |
| Amberlite IRC-718 | V | Rohm & Haas #6-2144 Lot# L-2-4902 | 4.103E-06 | 1.553E+03 | 1.084E+00 | 6.320E-03 | 7.788% |
| Resorcinol-Formaldehyde | W | BSC-187-210 | 3.829E-06 | 1.793E+03 | 1.162E+00 | 6.861E-03 | 13.953% |
| Amberlite CG-120 | X | Rohm & Haas #790-170 | 3.135E-06 | 4.467E+03 | 1.419E+00 | 1.400E-02 | 29.543% |
| Clinoptilolite | Y | Natural Zeolite | 3.721E-06 | 1.802E+03 | 1.196E+00 | 6.707E-03 | 16.372% |

3.3 Comparison of Simulated and Actual Waste Results

3.3.1 Cesium Batch Distribution

Figure 3.11 compares the average K_d (mL g⁻¹) results for cesium obtained from actual (NB0) and simulated (NB9) N-Basin water. The data are sorted by the material identification listing shown in Table 2.1. As is shown in the figure, several of the highest performance materials (e.g., KCoHex, TSP-137, phlogopite, modified biotites, IE-910, and IE-911) show a reduction in the cesium K_d value in the actual N-Basin water when compared to the simulated solution. In certain materials the difference between the average cesium K_d values is more than two orders of magnitude. The reason for the discrepancy is not known at this time but may be related to an incorrect simulant composition, the possible existence of recalcitrant or nonexchangeable cesium in the actual N-Basin water, or an analytical error that increases at higher K_d values. The observation is a significant concern when the data are integrated with those from

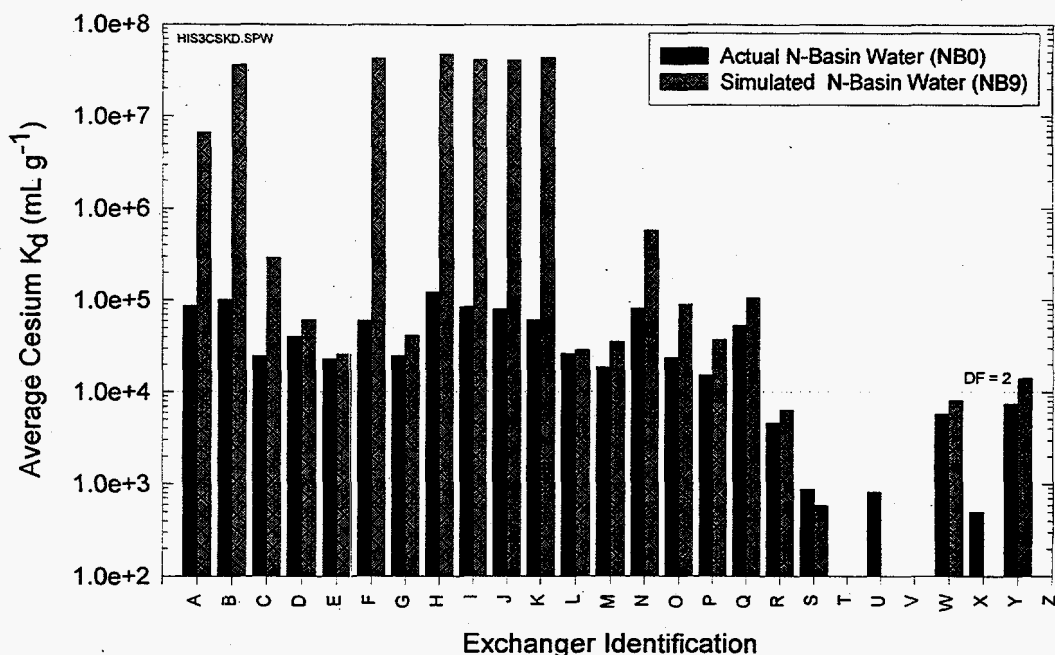


Figure 3.11. Comparison of Average Batch Distribution Coefficients for Cesium for 24 Ion Exchange Materials in Actual and Simulated 105 N-Basin Water

Figures 3.1 and 3.2. From these figures it is clear that, independent of the ion exchange material evaluated, the average cesium K_d for each individual material is nearly constant over several orders of magnitude in cesium concentration (e.g., from $1.0E-06$ to $1.0E-10$ M). Therefore, minor differences in the cesium concentration cannot explain the discrepancy.

Figure 3.12 compares the average loading (mmol g^{-1}) results for cesium obtained from actual (NB0) and simulated (NB9) N-Basin water. The data are sorted by the material identification listing shown in Table 2.1. As is shown in the figure, all of the materials show a slight increase in the cesium loading for the actual N-Basin water when compared to the simulated solution. This is a consequence of the slightly lower initial cesium concentration in the simulant ($2.57E-10$ M) when compared with the actual water ($4.87E-10$ M). In this case, the amount of cesium loaded on a particular ion exchange material is related to the concentration of cesium in solution, even though the cesium K_d is not affected. This effect was clearly demonstrated in Figure 3.5.

3.3.2 Strontium Batch Distribution

Figure 3.13 compares the average K_d (mL g^{-1}) results for strontium obtained from actual (NB0) and simulated (NB9) N-Basin water. The data are sorted by the material identification listing shown in Table 2.1. As is shown in the figure, most of the materials, including those with the highest performance (e.g., TSP-137, IE-910, IE-911, pharmacosiderite, Amberlite IRC-76) show a reduction in the strontium K_d

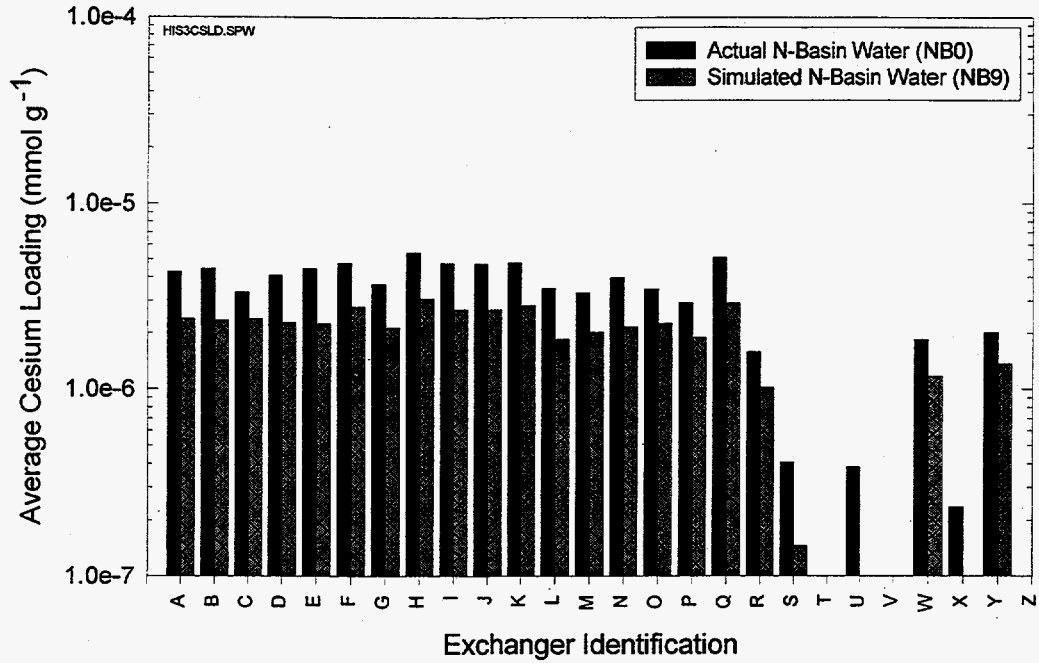


Figure 3.12. Comparison of Average Cesium Loadings for 24 Ion Exchange Materials in Actual and Simulated 105 N-Basin Water

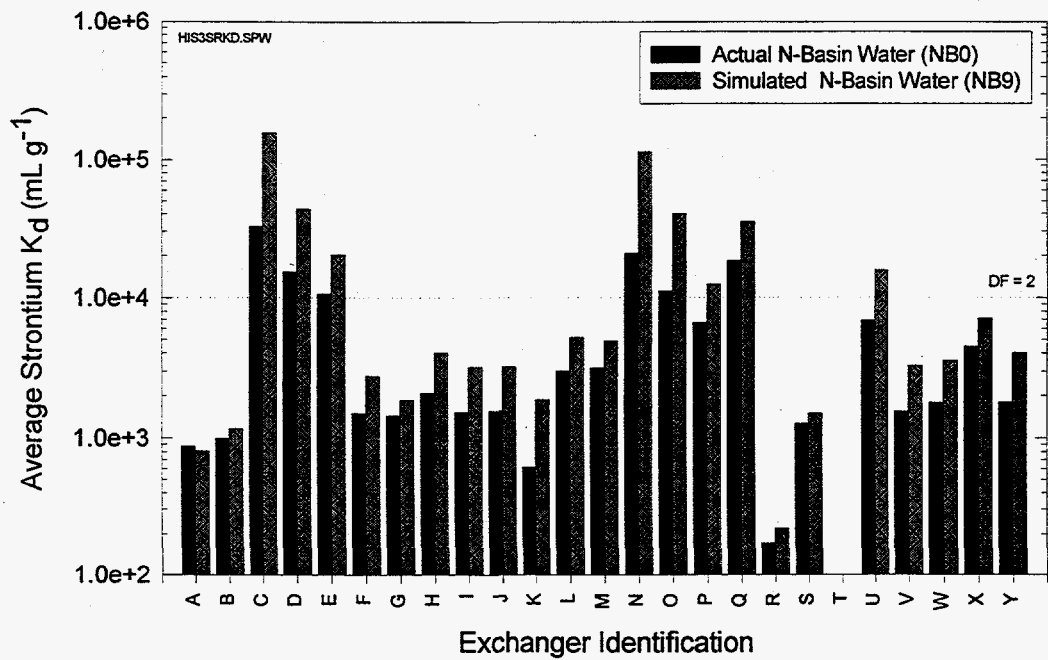


Figure 3.13. Comparison of Average Batch Distribution Coefficients for Strontium for 24 Ion Exchange Materials in Actual and Simulated 105 N-Basin Water

value in the actual N-Basin water when compared to the simulated solution. In some materials the difference between the average strontium K_d values is nearly an order of magnitude. The reason for the discrepancy is not known at this time but may be related to an incorrect simulant composition, the possible existence of recalcitrant or nonexchangeable strontium in the actual N-Basin water, or an analytical error that increases at higher K_d values.

Figure 3.14 compares the average loading (mmol g^{-1}) results for strontium obtained from actual (NB0) and simulated (NB9) N-Basin water. The data are sorted by the material identification listing shown in Table 2.1. As is shown in the figure, all of the materials exhibit a slight decrease in the strontium loading for the actual N-Basin water when compared to the simulated solution. This result is consistent with the previous strontium K_d data since the two values are directly correlated as described by Equation 2.1.

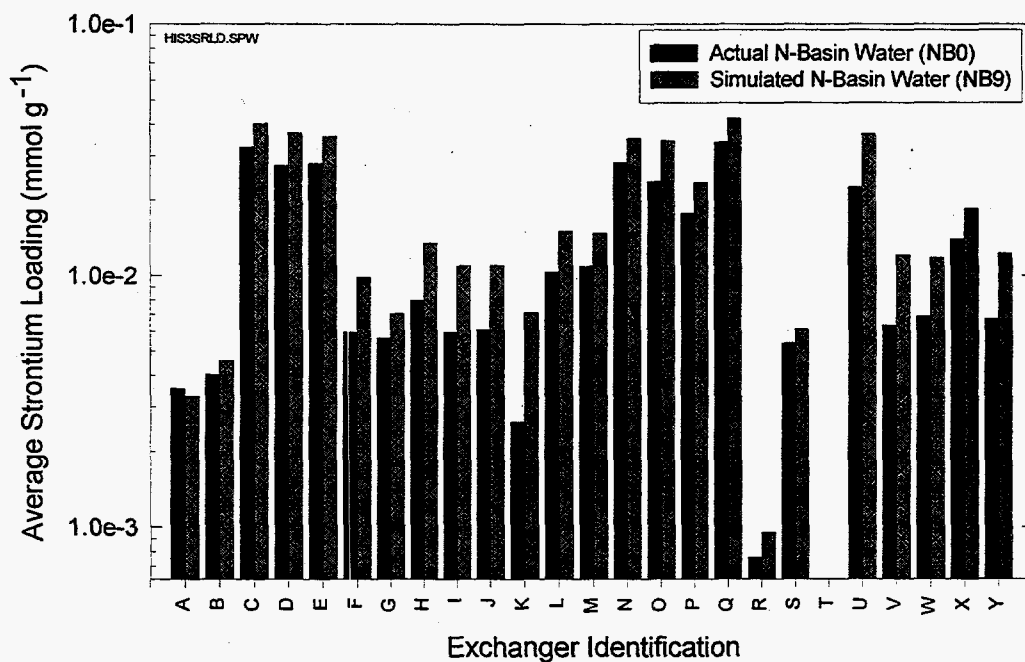


Figure 3.14. Comparison of Average Strontium Loadings for 24 Ion Exchange Materials in Actual and Simulated 105 N-Basin Water

4.0 Conclusions

This report evaluated 24 organic and inorganic ion exchange materials for their performance in removing cesium and strontium from actual and simulated waters from the 100-N area reactor basin at Hanford. The data described in this report can be applied to the development and evaluation of ion exchange pretreatment process flowsheets. Cesium and strontium batch distribution ratios (K_d s), decontamination factors (DF), and material loadings (mmol g^{-1}) are compared as a function of ion exchange material and initial cesium concentration.

The actual and simulated N-Basin waters contain relatively low levels of aluminum, barium, calcium, potassium, and magnesium (ranging from $8.33\text{E-}04$ to $6.40\text{E-}05$ M), with slightly higher levels of boron ($6.63\text{E-}03$ M) and sodium ($1.62\text{E-}03$ M). The ^{137}Cs level was $1.74\text{E-}06$ Ci L^{-1} which corresponds to approximately $4.87\text{E-}10$ M cesium. The initial Na/Cs ratio was $3.33\text{E+}06$. The concentration of total strontium was $4.45\text{E-}06$ M while the ^{90}Sr radioactive component was measured to be $6.13\text{E-}06$ Ci L^{-1} . Simulant tests were conducted using a stock solution with a variable initial cesium concentration ranging from $1.00\text{E-}04$ to $2.57\text{E-}10$ M cesium, with all other components held constant.

For all materials, the cesium uptake (as measured by the K_d) from simulated solutions increased with decreasing cesium concentration between $1.0\text{E-}04$ and $1.0\text{E-}07$ M cesium. Below about $1.0\text{E-}07$ M, the cesium uptake did not change, irrespective of the cesium concentration. Cesium K_d values exceeding $1.0\text{E+}07$ mL g^{-1} were measured in the simulated N-Basin waters. Several materials, including potassium cobalt hexacyanoferrate (KCoHex), crystalline silicotitanates, biotite micas, pharmacosiderites, phlogopites, and inorganic zeolites, showed substantial affinity for cesium. Nonspecific cation exchange materials did not show an appreciable affinity for cesium in the basin water. In contrast to the K_d results, material loading (mmol Cs g^{-1}) was nearly proportional to the equilibrium cesium concentration. The data suggest that accurately predicting material performance using this batch distribution method requires multiple solutions with a wide range of initial cesium concentrations.

TSP-137, produced by Texas A&M, yielded the highest strontium K_d values in the actual N-Basin water followed by IE-910 and IE-911 produced by UOP, two pharmacosiderites produced by Texas A&M, and Amberlite IRC-76 produced by Rohm & Haas.

The strontium K_d and loading were inversely correlated to the cesium concentration (increasing with decreasing concentration from $1.0\text{E-}04$ to $1.0\text{E-}09$ M cesium). The data suggest that either the two ions compete for similar ion exchange sites or the higher cesium loading perturbs the strontium sites such that the strontium exchange process is hindered.

In nearly all of the ion exchange materials tested, the cesium and strontium values obtained when using the actual N-Basin water were lower than those obtained from simulated solutions. These data emphasize the importance of authenticating ion exchanger performance using actual wastes when possible. In certain materials the difference between the average cesium K_d values was more than two orders of magnitude.

The reason for the discrepancy is not known but may be related to an incorrect simulant composition, the possible existence of recalcitrant or nonexchangeable cesium in the actual N-Basin water, or an analytical error that increases at higher K_d values.

5.0 References

Anthony, R. G., R. G. Dosch, D. Gu and C. V. Philip. 1994. "Use of Silico-Titanates for Removing Cesium and Strontium from Defense Waste," *I&EC Research*, 33 (11), 2702-5.

Anthony, R. G., C. V. Philip, and R. G. Dosch. 1993. "Selective Adsorption and Ion Exchange of Metal Cations and Anions with Silico-Titanates and Layered Titanates," *Waste Management*, 13, 503.

Bibler, J. P. 1994. *Year-End Report for UST: Cesium Extraction Testing Project DOE/DT&E TTP No. SR1-03-20-01 (U)*, WSRC-RP-94-146, Westinghouse Savannah River Company, Aiken, South Carolina.

Bibler, J. P. 1991. *A Comparison of Duolite™ CS-100 and SRS Resorcinol/Formaldehyde Ion Exchange Resins with Three High-Level Waste Simulants Before and After γ -Irradiation*, WSRC-RP-91-1221, Westinghouse Savannah River Company, Aiken, South Carolina.

Bibler, N. E. and C. L. Crawford. 1994. *An Investigation of the Radiolytic Stability of a Resorcinol-Formaldehyde Ion Exchange Resin*, WSRC-RP-94-148, Westinghouse Savannah River Company, Aiken, South Carolina.

Bibler, J. P., R. M. Wallace, and L. A. Bray. 1989. "Testing A New Cesium-Specific Ion Exchange Resin For Decontamination of Alkaline-High Activity Waste." In *Proceedings of the Symposium on Waste Management '90*, February 25 - March 1, 1990. Tucson, Arizona.

Bray, L. A., J. E. Amonette, G. N. Brown, T. M. Kafka, and S. F. Yates. 1995a. *Efficient Separations and Processing Crosscutting Program: Develop and Test Sorbents*. PNL-10750, Pacific Northwest Laboratory, Richland, Washington.

Bray, L. A., G. N. Brown, D. R. Anderson, L. R. White, T. M. Kafka, R. L. Bruening, R. H. Decker, L. C. Lewis, and C. W. Lundholm. 1995b. *Web Technology in the Separation of Strontium and Cesium from INEL-ICPP Radioactive Acid Waste (WM-185)*. PNL-10283, Pacific Northwest Laboratory, Richland, Washington.

Bray, L. A., C. D. Carlson, K. J. Carson, J. R. DesChane, R. J. Elovich and D. E. Kurath. 1993a. *Initial Evaluation of Two Organic Resins and their Ion Exchange Column Performance for the Recovery of Cesium from Hanford Alkaline Wastes*. TWRSP-93-055, Pacific Northwest National Laboratory, Richland, Washington.

Bray, L. A., K. J. Carson, and R. J. Elovich. 1993b. *Initial Evaluation of Sandia National Laboratory Prepared Crystalline Silico-Titanates for the Recovery of Cesium*. PNL-8847, Pacific Northwest National Laboratory, Richland, Washington.

Bray, L. A., K. J. Carson, R. J. Elovich, and D. E. Kurath. 1992. *Equilibrium Data for Cesium Ion Exchange of Hanford CC and NCAW Tank Waste*. TWRSP-92-020, Pacific Northwest National Laboratory, Richland, Washington.

Bray, L. A. and F. T. Hara. 1991. "Use of Titanium-Treated Zeolite for Plutonium, Strontium, and Cesium Removal from West Valley Alkaline Wastes and Sludge Wash Waters." In *First Hanford Separations Science Workshop*. PNL-SA-19697S, pp. II.87-II.91. Pacific Northwest National Laboratory, Richland, Washington.

Bray, L. A., K. J. Carson, and R. J. Elovich. 1990. *Cesium Recovery Using Savannah River Laboratory Resorcinol-Formaldehyde Ion Exchange Resin*. PNL-7273, Pacific Northwest National Laboratory, Richland, Washington.

Bray, L. A., L. K. Holton, T. R. Meyers, G. M. Richardson, and B. M. Wise. 1984. *Experimental Data Developed to Support the Selection of a Treatment Process for West Valley Alkaline Supernatant*. PNL-4969, Pacific Northwest National Laboratory, Richland, Washington.

Brown, G. N., J. E. Amonette, T. M. Kafka (3M), and S. F. Yates (AlliedSignal). 1996a. *FY 1996 Annual Progress Report from October 1, 1995 to September 30, 1996. Efficient Separations and Processing Crosscutting Program: Develop and Test Sorbents*. PNNL-11451, Pacific Northwest National Laboratory, Richland, Washington.

Brown, G. N., L. A. Bray, C. D. Carlson, K. J. Carson, J. R. DesChane, R. J. Elovich, F. V. Hoopes, D. E. Kurath, L. L. Nenninger, and P. K. Tanaka. 1996b. *Comparison of Organic and Inorganic Ion Exchangers for Removal of Cesium and Strontium from Simulated and Actual Hanford 241-AW-101 DSSF Tank Waste*. PNL-10920, Pacific Northwest National Laboratory, Richland, Washington.

Brown, G. N., K. J. Carson, J. R. DesChane, R. J. Elovich, and P. K. Berry. 1996c. *Chemical and Radiation Stability of a Proprietary Cesium Ion Exchange Material Manufactured from WWL Membrane and SuperLig®644*. PNNL-11328, Pacific Northwest National Laboratory, Richland, Washington.

Brown, G. N., K. J. Carson, J. R. DesChane, R. J. Elovich, T. M. Kafka, and L. R. White. 1996d. *Ion Exchange Removal of Strontium from Simulated and Actual N-Springs Well Water at the Hanford 100-N Area*. PNL-11198, Pacific Northwest National Laboratory, Richland, Washington.

Brown, G. N., S. R. Adami, L. A. Bray, S. A. Bryan, C. D. Carlson, K. J. Carson, J. R. DesChane, R. J. Elovich, S. J. Forbes, J. A. Franz, J. C. Linehan, W. J. Shaw, P. K. Tanaka, and M. R. Telander. 1995a. *Chemical and Radiation Stability of SuperLig® 644, Resorcinol-Formaldehyde, and CS-100 Cesium Ion Exchange Materials*. PNL-10772, Pacific Northwest National Laboratory, Richland, Washington.

Brown, G. N., J. R. Bontha, C. D. Carlson, K. J. Carson, J. R. DesChane, R. J. Elovich, D. E. Kurath, P. K. Tanaka, D. W. Edmonson, D. L. Herting, and J. R. Smith. 1995b. *Ion Exchange Removal of Cesium from Simulated and Actual Supernate from Hanford Tanks 241-SY-101 and 241-SY-103*. PNL-10792, Pacific Northwest National Laboratory, Richland, Washington.

Brown, G. N., L. A. Bray, R. J. Elovich. 1995c. *Evaluation and Comparison of SuperLig® 644, Resorcinol-Formaldehyde and CS-100 Ion Exchange Materials for the Removal of Cesium from Simulated Alkaline Supernate*. PNL-10486, Pacific Northwest National Laboratory, Richland, Washington.

Buckingham, J. S. 1967. *Waste Management Technical Manual*. ISO-100 DEL, Hanford Atomic Products Operation, Richland, Washington.

Carlson, C. D., L. A. Bray, S. A. Bryan, J. A. Franz, D. E. Kurath, S. R. Adami, G. N. Brown, J. R. DesChane, R. J. Elovich, J. C. Linehan, W. S. Shaw, and M. R. Telander. 1995. *Radiation Testing of Organic Ion Exchange Resins*. PNL-10767, Pacific Northwest National Laboratory, Richland, Washington.

Dosch, R. G., N. E. Brown, H. P. Stephens, and R. G. Anthony. 1993. "Treatment of Liquid Nuclear Wastes with Advanced Forms of Titanate Ion Exchangers," Waste Management '93, 1751, Tucson, Arizona.

Eager, K. M., D. L. Penwell, and B. J. Knutson. 1994. *Preliminary Flowsheet: Ion Exchange Process for Separation of Cesium from Hanford Tank Waste Using Duolite CS-100 Resin*. WHC-SD-WM-TI-667 Rev. 0, Westinghouse Hanford Company, Richland, Washington.

Fong, L. and M. Hyman. 1995. *105 N-Basin and Emergency Dump Basin Liquid Effluent Treatment*. BHI-00647, Rev. 0, Bechtel Hanford Incorporated, Richland, Washington

Greenidge, M. E. 1995. *105N Basin Liquid Effluent Treatment Options*. BHI-00258, Rev. 0, Bechtel Hanford Incorporated, Richland, Washington.

Herbst, R. S., K. N. Brewer, T. A. Todd, T. M. Kafka, L. R. White, and L. A. Bray. 1995. *Decontamination of TAN Injection Well Water Using 3M Web Technology*. INEL-95/0589. Lockheed Idaho Technologies Company, Idaho Falls, Idaho.

Hubler, T. L., J. A. Franz, W. J. Shaw, M. O. Hogan, R. T. Hallen, G. N. Brown, and J. C. Linehan. 1996a. *Structure/Function Studies of Resorcinol-Formaldehyde (R-F) and Phenol-Formaldehyde (P-F) Copolymer Ion-Exchange Resins*. PNNL-11347, Pacific Northwest National Laboratory, Richland, Washington.

Hubler, T. L., W. J. Shaw, G. N. Brown, J. C. Linehan, J. A. Franz, T. R. Hart, M. O. Hogen. 1996b. *Chemical Derivation to Enhance the Chemical/Oxidative Stability of Resorcinol-Formaldehyde (R-F) Resin*. PNNL-11327, Pacific Northwest National Laboratory, Richland, Washington.

Hubler, T. L., J. A. Franz, W. J. Shaw, S. A. Bryan, R. T. Hallen, G. N. Brown, L. A. Bray, and J. C. Linehan. 1995. *Synthesis, Structural Characterization, and Performance of Resorcinol-Formaldehyde (R-F) Ion-Exchange Resin*. PNL-10744, Pacific Northwest Laboratory, Richland, Washington.

Hunacek, G. S. 1992. *N Reactor Effluent Treatment Technology Study*. WHC-SD-NR-ES-013, Rev. 0, Westinghouse Hanford Company, Richland, Washington.

Klavetter, E. A., N. E. Brown, D. E. Trudell, R. G. Anthony, D. Gu, and C. Thibaud-Erkey. 1994. "Ion-Exchange Performance of Crystalline Silicotitanates for Cesium Removal from Hanford Tank Waste Simulants," *Waste Management '94*, 709, Tucson, AZ.

Kurath, D. E., L. A. Bray, K. P. Brooks, G. N. Brown, S. A. Bryan, C. D. Carlson, K. J. Carson, J. R. DesChane, R. J. Elovich and A. Y. Kim. 1994. *Experimental Data and Analysis to Support the Design of an Ion Exchange Process for the Treatment of Hanford Tank Waste Supernatant Liquids*. PNL-10187, Pacific Northwest Laboratory, Richland, Washington.

Marsh, S. F., Z. V. Svitra, and S. M. Bowen. 1995. *Effects of Soluble Organic Complexants and Their Degradation Products on the Removal of Selected Radionuclides from High-Level Waste*. LA-13000, Los Alamos National Laboratory, Los Alamos, New Mexico.

Marsh, S. F., Z. V. Svitra, and S. M. Bowen. 1994. *Distributions of 15 Elements on 58 Absorbers from Simulated Hanford Double-Shell Slurry Feed (DSSF)*. LA-12863, Los Alamos National Laboratory, Los Alamos, New Mexico.

Miller, J. E. and N. E. Brown. 1997. *Development and Properties of Crystalline Silicotitanate (CST) Ion Exchangers for Radioactive Waste Applications*. SAND97-0771. Sandia National Laboratories, Albuquerque, New Mexico.

Orme, R. M. 1995. *TWRS Process Flow Sheet*. WHC-SD-WM-TI-613, Rev 1. Westinghouse Hanford Company, Richland, Washington.

Penwell, D. L., K. M. Eager, and B. J. Knutson. 1994. *Preliminary Flowsheet: Ion Exchange Process for Separation of Cesium from Hanford Tank Waste Using Resorcinol-Formaldehyde Resin*. WHC-SD-WM-TI-638 Rev. 0, Westinghouse Hanford Company, Richland, Washington.

Samuelson, O. 1963. *Ion Exchanger Separations in Analytical Chemistry*. John Wiley and Sons, New York.

Samuelson, O. 1953. *Ion Exchangers in Analytical Chemistry*. John Wiley and Sons, New York.

Svitra, Z. V., S. F. Marsh, and S. M. Bowen. 1994. *Distributions of 12 Elements on 64 Absorbers from Simulated Hanford Neutralized Current Acid Waste (NCAW)*. LA-12889, Los Alamos National Laboratory, Los Alamos, New Mexico.

Van Vleet. 1993. *Radionuclide and Chemical Inventories For the Double Shell Tanks*. WHC-SD-WM-TI-543 Rev. 1, Westinghouse Hanford Company, Richland, Washington.

Zheng, Z., D. Gu, R. G. Anthony, and E. A. Klavetter. 1995. "Estimation of Cesium Ion Exchange Distribution Coefficient for Concentrated Electrolytic Solutions When Using Crystalline Silicotitanates," *I&EC Research*, 34(6), 2142-2147.

Appendix A

Data Set for All Materials Tested

| ID Number | A4-1 | A4-2 | B4-1 | B4-2 | C4-1 | C4-2 | D4-1 | D4-2 | E4-1 | E4-2 | F4-1 | F4-2 | G4-1 | G4-2 | H4-1 | H4-2 |
|--------------------|---------------------------|-----------|--------------------------|-----------|---------------|-----------|-------------------|-----------|-------------------|-----------|--------------------------|-----------|----------------------|-----------|-------------------------|-----------|
| Material | 3M #2999-14 CoHex unmilld | | 3M #2999-14 CoHex milled | | TAMU #TSP-137 | | TAMU #E-B Pharm-1 | | TAMU #E-B Pharm-2 | | TAMU #Phlogopite 90% Na+ | | TAMU Biotite 60% Na+ | | AS #8212-32A Zr-Biotite | |
| Cs Kd (ml/g) | 6.308E+03 | 6.775E+03 | 1.461E+04 | 1.466E+04 | 3.759E+04 | 3.793E+04 | 2.781E+04 | 2.790E+04 | 1.199E+04 | 1.603E+04 | 4.451E+04 | 5.766E+04 | 4.810E+03 | 5.119E+03 | 7.432E+03 | 8.118E+03 |
| Load (mmol/g) | 3.879E-01 | 4.038E-01 | 5.881E-01 | 6.057E-01 | 7.899E-01 | 7.957E-01 | 7.819E-01 | 7.928E-01 | 6.414E-01 | 7.589E-01 | 8.877E-01 | 9.604E-01 | 3.338E-01 | 3.506E-01 | 4.662E-01 | 4.879E-01 |
| Initial [Cs] (M) | 1.000E-04 | 1.000E-04 | 1.000E-04 | 1.000E-04 | 1.000E-04 | 1.000E-04 | 1.000E-04 | 1.000E-04 | 1.000E-04 | 1.000E-04 | 1.000E-04 | 1.000E-04 | 1.000E-04 | 1.000E-04 | 1.000E-04 | 1.000E-04 |
| Final [Cs] (M) | 6.149E-05 | 5.961E-05 | 4.025E-05 | 4.132E-05 | 2.101E-05 | 2.097E-05 | 2.812E-05 | 2.841E-05 | 5.349E-05 | 4.736E-05 | 1.994E-05 | 1.866E-05 | 6.940E-05 | 6.850E-05 | 6.273E-05 | 6.010E-05 |
| DF (Initial/Final) | 1.626E+00 | 1.678E+00 | 2.484E+00 | 2.420E+00 | 4.759E+00 | 4.768E+00 | 3.557E+00 | 3.519E+00 | 1.869E+00 | 2.112E+00 | 5.014E+00 | 6.004E+00 | 1.441E+00 | 1.460E+00 | 1.594E+00 | 1.664E+00 |
| % Removal | 38.51% | 40.39% | 59.75% | 58.68% | 78.99% | 79.03% | 71.88% | 71.59% | 46.51% | 52.64% | 80.06% | 83.34% | 30.60% | 31.50% | 37.27% | 39.90% |
| ID Number | A5-1 | A5-2 | B5-1 | B5-2 | C5-1 | C5-2 | D5-1 | D5-2 | E5-1 | E5-2 | F5-1 | F5-2 | G5-1 | G5-2 | H5-1 | H5-2 |
| Material | 3M #2999-14 CoHex unmilld | | 3M #2999-14 CoHex milled | | TAMU #TSP-137 | | TAMU #E-B Pharm-1 | | TAMU #E-B Pharm-2 | | TAMU #Phlogopite 90% Na+ | | TAMU Biotite 60% Na+ | | AS #8212-32A Zr-Biotite | |
| Cs Kd (ml/g) | 7.739E+05 | 3.844E+05 | 3.803E+07 | 3.158E+06 | 1.417E+05 | 1.069E+05 | 7.479E+04 | 4.689E+04 | 3.073E+04 | 3.223E+04 | 5.703E+05 | 5.671E+05 | 2.496E+04 | 3.119E+04 | 1.666E+04 | 1.982E+04 |
| Load (mmol/g) | 9.334E-02 | 9.740E-02 | 1.031E-01 | 1.028E-01 | 8.915E-02 | 9.307E-02 | 9.911E-02 | 8.615E-02 | 9.959E-02 | 1.013E-01 | 1.159E-01 | 1.137E-01 | 7.635E-02 | 8.010E-02 | 7.019E-02 | 7.417E-02 |
| Initial [Cs] (M) | 1.000E-05 | 1.000E-05 | 1.000E-05 | 1.000E-05 | 1.000E-05 | 1.000E-05 | 1.000E-05 | 1.000E-05 | 1.000E-05 | 1.000E-05 | 1.000E-05 | 1.000E-05 | 1.000E-05 | 1.000E-05 | 1.000E-05 | 1.000E-05 |
| Final [Cs] (M) | 1.220E-07 | 2.547E-07 | 1.084E-08 | 3.255E-08 | 6.292E-07 | 8.706E-07 | 1.325E-06 | 1.837E-06 | 3.241E-06 | 3.144E-06 | 2.033E-07 | 2.005E-07 | 3.059E-06 | 2.568E-06 | 4.212E-06 | 3.743E-06 |
| DF (Initial/Final) | 8.200E+01 | 3.928E+01 | 9.225E+02 | 3.073E+02 | 1.589E+01 | 1.149E+01 | 7.546E+00 | 5.442E+00 | 3.085E+00 | 3.181E+00 | 4.920E+01 | 4.986E+01 | 3.289E+00 | 3.894E+00 | 2.374E+00 | 2.672E+00 |
| % Removal | 98.79% | 97.47% | 99.97% | 99.67% | 93.71% | 91.29% | 86.75% | 81.63% | 67.59% | 68.66% | 97.97% | 97.99% | 69.41% | 74.32% | 67.88% | 62.57% |
| ID Number | A6-1 | A6-2 | B6-1 | B6-2 | C6-1 | C6-2 | D6-1 | D6-2 | E6-1 | E6-2 | F6-1 | F6-2 | G6-1 | G6-2 | H6-1 | H6-2 |
| Material | 3M #2999-14 CoHex unmilld | | 3M #2999-14 CoHex milled | | TAMU #TSP-137 | | TAMU #E-B Pharm-1 | | TAMU #E-B Pharm-2 | | TAMU #Phlogopite 90% Na+ | | TAMU Biotite 60% Na+ | | AS #8212-32A Zr-Biotite | |
| Cs Kd (ml/g) | 1.917E+06 | 2.325E+05 | 3.599E+06 | 1.568E+07 | 2.968E+05 | 4.686E+05 | 6.601E+04 | 5.768E+04 | 1.682E+04 | 2.659E+04 | 3.521E+04 | 3.555E+04 | 1.121E+03 | 1.053E+03 | 1.656E+04 | 1.898E+04 |
| Load (mmol/g) | 9.813E-03 | 9.606E-03 | 1.032E-02 | 9.768E-03 | 9.510E-03 | 9.879E-03 | 9.433E-03 | 9.310E-03 | 7.690E-03 | 9.681E-03 | 8.580E-03 | 8.910E-03 | 1.020E-03 | 9.655E-04 | 7.119E-03 | 7.339E-03 |
| Initial [Cs] (M) | 1.000E-06 | 1.000E-06 | 1.000E-06 | 1.000E-06 | 1.000E-06 | 1.000E-06 | 1.000E-06 | 1.000E-06 | 1.000E-06 | 1.000E-06 | 1.000E-06 | 1.000E-06 | 1.000E-06 | 1.000E-06 | 1.000E-06 | 1.000E-06 |
| Final [Cs] (M) | 5.118E-09 | 4.132E-08 | 2.868E-09 | 6.235E-10 | 3.206E-08 | 2.108E-08 | 1.429E-07 | 1.614E-07 | 4.572E-07 | 3.640E-07 | 2.436E-07 | 2.506E-07 | 9.101E-07 | 9.168E-07 | 4.299E-07 | 3.867E-07 |
| DF (Initial/Final) | 1.954E+02 | 2.420E+01 | 3.487E+02 | 1.604E+03 | 3.119E+01 | 4.744E+01 | 6.998E+00 | 6.196E+00 | 2.187E+00 | 2.747E+00 | 4.104E+00 | 3.990E+00 | 1.099E+00 | 1.091E+00 | 2.326E+00 | 2.586E+00 |
| % Removal | 99.49% | 95.87% | 99.71% | 99.94% | 96.79% | 97.89% | 85.71% | 83.86% | 54.28% | 63.60% | 75.64% | 74.94% | 8.99% | 8.32% | 67.01% | 61.33% |
| ID Number | A7-1 | A7-2 | B7-1 | B7-2 | C7-1 | C7-2 | D7-1 | D7-2 | E7-1 | E7-2 | F7-1 | F7-2 | G7-1 | G7-2 | H7-1 | H7-2 |
| Material | 3M #2999-14 CoHex unmilld | | 3M #2999-14 CoHex milled | | TAMU #TSP-137 | | TAMU #E-B Pharm-1 | | TAMU #E-B Pharm-2 | | TAMU #Phlogopite 90% Na+ | | TAMU Biotite 60% Na+ | | AS #8212-32A Zr-Biotite | |
| Cs Kd (ml/g) | 3.881E+05 | 4.752E+05 | 2.561E+07 | 1.155E+07 | 3.399E+05 | 2.120E+05 | 6.726E+04 | 5.920E+04 | 2.872E+04 | 2.256E+04 | 4.153E+04 | 3.651E+04 | 8.429E+02 | 1.016E+03 | 1.860E+04 | 1.921E+04 |
| Load (mmol/g) | 9.673E-04 | 9.416E-04 | 9.797E-04 | 1.031E-03 | 9.317E-04 | 9.000E-04 | 9.699E-04 | 9.624E-04 | 9.806E-04 | 8.709E-04 | 9.133E-04 | 8.600E-04 | 7.829E-05 | 9.291E-05 | 7.399E-04 | 7.917E-04 |
| Initial [Cs] (M) | 1.000E-07 | 1.000E-07 | 1.000E-07 | 1.000E-07 | 1.000E-07 | 1.000E-07 | 1.000E-07 | 1.000E-07 | 1.000E-07 | 1.000E-07 | 1.000E-07 | 1.000E-07 | 1.000E-07 | 1.000E-07 | 1.000E-07 | 1.000E-07 |
| Final [Cs] (M) | 2.493E-09 | 1.981E-09 | 3.825E-11 | 8.925E-11 | 2.741E-09 | 4.246E-09 | 1.442E-08 | 1.626E-08 | 3.394E-08 | 3.861E-08 | 2.199E-08 | 2.355E-08 | 9.288E-08 | 9.145E-08 | 3.977E-08 | 4.120E-08 |
| DF (Initial/Final) | 4.012E+01 | 5.047E+01 | 2.614E+03 | 1.120E+03 | 3.648E+01 | 2.355E+01 | 6.935E+00 | 6.151E+00 | 2.947E+00 | 2.590E+00 | 4.547E+00 | 4.246E+00 | 1.077E+00 | 1.094E+00 | 2.514E+00 | 2.427E+00 |
| % Removal | 97.51% | 98.02% | 99.96% | 99.91% | 97.26% | 95.75% | 85.68% | 83.74% | 66.06% | 61.39% | 78.01% | 76.45% | 7.12% | 8.55% | 60.23% | 58.80% |
| ID Number | A8-1 | A8-2 | B8-1 | B8-2 | C8-1 | C8-2 | D8-1 | D8-2 | E8-1 | E8-2 | F8-1 | F8-2 | G8-1 | G8-2 | H8-1 | H8-2 |
| Material | 3M #2999-14 CoHex unmilld | | 3M #2999-14 CoHex milled | | TAMU #TSP-137 | | TAMU #E-B Pharm-1 | | TAMU #E-B Pharm-2 | | TAMU #Phlogopite 90% Na+ | | TAMU Biotite 60% Na+ | | AS #8212-32A Zr-Biotite | |
| Cs Kd (ml/g) | 7.913E+05 | 1.586E+06 | 2.826E+06 | 2.656E+07 | 4.495E+05 | 4.408E+05 | 6.647E+04 | 4.716E+04 | 2.917E+04 | 2.572E+04 | 1.297E+04 | 1.064E+04 | 2.541E+03 | 2.610E+03 | 1.602E+05 | 7.242E+04 |
| Load (mmol/g) | 9.465E-05 | 9.686E-05 | 9.715E-05 | 1.014E-04 | 9.794E-05 | 9.715E-05 | 9.437E-05 | 8.883E-05 | 9.863E-05 | 9.238E-05 | 6.134E-05 | 5.426E-05 | 2.064E-05 | 2.106E-05 | 1.121E-04 | 1.034E-04 |
| Initial [Cs] (M) | 1.000E-08 | 1.000E-08 | 1.000E-08 | 1.000E-08 | 1.000E-08 | 1.000E-08 | 1.000E-08 | 1.000E-08 | 1.000E-08 | 1.000E-08 | 1.000E-08 | 1.000E-08 | 1.000E-08 | 1.000E-08 | 1.000E-08 | 1.000E-08 |
| Final [Cs] (M) | 1.196E-10 | 6.108E-11 | 3.437E-11 | 3.819E-12 | 2.179E-10 | 2.204E-10 | 1.420E-09 | 1.884E-09 | 3.399E-09 | 3.592E-09 | 4.730E-09 | 5.097E-09 | 8.123E-09 | 8.069E-09 | 6.997E-10 | 1.427E-09 |
| DF (Initial/Final) | 8.360E+01 | 1.637E+02 | 2.909E+02 | 2.618E+03 | 4.590E+01 | 4.537E+01 | 7.043E+00 | 5.309E+00 | 2.942E+00 | 2.784E+00 | 2.114E+00 | 1.962E+00 | 1.231E+00 | 1.239E+00 | 1.429E+01 | 7.005E+00 |
| % Removal | 98.80% | 99.39% | 99.66% | 99.96% | 97.82% | 97.80% | 85.80% | 81.16% | 66.01% | 64.08% | 62.70% | 49.03% | 18.77% | 19.31% | 93.00% | 85.73% |
| ID Number | A9-1 | A9-2 | B9-1 | B9-2 | C9-1 | C9-2 | D9-1 | D9-2 | E9-1 | E9-2 | F9-1 | F9-2 | G9-1 | G9-2 | H9-1 | H9-2 |
| Material | 3M #2999-14 CoHex unmilld | | 3M #2999-14 CoHex milled | | TAMU #TSP-137 | | TAMU #E-B Pharm-1 | | TAMU #E-B Pharm-2 | | TAMU #Phlogopite 90% Na+ | | TAMU Biotite 60% Na+ | | AS #8212-32A Zr-Biotite | |
| Cs Kd (ml/g) | 3.996E+05 | 1.303E+07 | 3.680E+07 | 3.606E+07 | 2.959E+05 | 2.909E+05 | 6.103E+04 | 6.204E+04 | 2.104E+04 | 3.092E+04 | 4.308E+07 | 4.307E+07 | 4.187E+04 | 4.128E+04 | 4.667E+07 | 4.871E+07 |
| Load (mmol/g) | 2.273E-06 | 2.526E-06 | 2.378E-06 | 2.300E-06 | 2.390E-06 | 2.406E-06 | 2.291E-06 | 2.281E-06 | 2.126E-06 | 2.382E-06 | 2.784E-06 | 2.783E-06 | 2.189E-06 | 2.086E-06 | 3.148E-06 | 3.148E-06 |
| Initial [Cs] (M) | 2.570E-10 | 2.570E-10 | 2.570E-10 | 2.570E-10 | 2.570E-10 | 2.570E-10 | 2.570E-10 | 2.570E-10 | 2.570E-10 | 2.570E-10 | 2.570E-10 | 2.570E-10 | 2.570E-10 | 2.570E-10 | 2.570E-10 | 2.570E-10 |
| Final [Cs] (M) | 5.687E-12 | 1.939E-13 | 6.462E-14 | 6.462E-14 | 8.078E-12 | 8.272E-12 | 3.755E-11 | 3.677E-11 | 1.000E-10 | 7.703E-11 | 6.462E-14 | 6.462E-14 | 5.228E-11 | 5.053E-11 | 6.462E-14 | 6.462E-14 |
| DF (Initial/Final) | 4.519E+01 | 1.326E+03 | 3.977E+03 | 3.977E+03 | 3.182E+01 | 3.107E+01 | 6.845E+00 | 6.989E+00 | 2.569E+00 | 3.336E+00 | 3.977E+03 | 3.977E+03 | 4.916E+00 | 5.086E+00 | 3.977E+03 | 3.977E+03 |
| % Removal | 97.79% | 99.92% | 99.97% | 99.97% | 96.86% | 96.78% | 85.39% | 85.69% | 61.08% | 70.03% | 99.97% | 99.97% | 79.66% | 80.34% | 99.97% | 99.97% |
| ID Number | A0-1 | A0-2 | B0-1 | B0-2 | C0-1 | C0-2 | D0-1 | D0-2 | E0-1 | E0-2 | F0-1 | F0-2 | G0-1 | G0-2 | H0-1 | H0-2 |
| Material | 3M #2999-14 CoHex unmilld | | 3M #2999-14 CoHex milled | | TAMU #TSP-137 | | TAMU #E-B Pharm-1 | | TAMU #E-B Pharm-2 | | TAMU #Phlogopite 90% Na+ | | TAMU Biotite 60% Na+ | | AS #8212-32A Zr-Biotite | |
| Cs Kd (ml/g) | 9.052E+04 | 8.510E+04 | 9.455E+04 | 1.099E+05 | 2.304E+04 | 2.627E+04 | 5.826E+04 | 2.332E+04 | 2.178E+04 | 2.407E+04 | 6.002E+04 | 6.099E+04 | 2.678E+04 | 2.293E+04 | 1.240E+05 | 1.231E+05 |
| Load (mmol/g) | 4.269E-06 | 4.273E-06 | 4.333E-06 | 4.537E-06 | 3.302E-06 | 3.368E-06 | 4.530E-06 | 3.674E-06 | 4.368E-06 | 4.533E-06 | 4.760E-06 | 4.758E-06 | 3.785E-06 | 3.549E-06 | 5.517E-06 | 5.448E-06 |
| Initial [Cs] (M) | 4.870E-10 | 4.870E-10 | 4.870E-10 | 4.870E-10 | 4.870E-10 | 4.870E-10 | 4.870E-10 | 4.870E-10 | 4.870E-10 | 4.870E-10 | 4.870E-10 | 4.870E-10 | 4.870E-10 | 4.870E-10 | 4.870E-10 | 4.870E-10 |
| Final [Cs] (M) | 4.716E-11 | 5.021E-11 | 4.583E-11 | 4.127E-11 | 1.433E-10 | 1.282E-10 | 7.77 | | | | | | | | | |

| ID Number | A4-1 | A4-2 | B4-1 | B4-2 | C4-1 | C4-2 | D4-1 | D4-2 | E4-1 | E4-2 | F4-1 | F4-2 | G4-1 | G4-2 | H4-1 | H4-2 |
|------------------|---------------------------|-----------|--------------------------|-----------|---------------|-----------|-------------------|-----------|-------------------|-----------|--------------------------|-----------|----------------------|-----------|-------------------------|-----------|
| Material | 3M #2999-14 CoHex unmlled | | 3M #2999-14 CoHex milled | | TAMU #TSP-137 | | TAMU #E-B Pharm-1 | | TAMU #E-B Pharm-2 | | TAMU #Phlogopite 90% Na+ | | TAMU Biotite 60% Na+ | | AS #8212-32A Zr-Biotite | |
| Sr Kd (mL/g) | 6.499E+02 | 7.915E+02 | 1.140E+03 | 8.864E+02 | 1.200E+04 | 1.212E+04 | 2.155E+04 | 1.889E+04 | 8.493E+03 | 1.056E+04 | 2.389E+03 | 3.077E+03 | 3.739E+02 | 5.990E+02 | 1.721E+03 | 1.955E+03 |
| Load (mmol/g) | 2.717E-03 | 3.264E-03 | 4.545E-03 | 3.633E-03 | 2.427E-02 | 2.448E-02 | 3.217E-02 | 3.107E-02 | 2.339E-02 | 2.713E-02 | 8.746E-03 | 1.081E-02 | 3.075E-03 | 2.530E-03 | 6.733E-03 | 7.500E-03 |
| Initial [Sr] (M) | 4.450E-06 | 4.450E-06 | 4.450E-06 | 4.450E-06 | 4.450E-06 | 4.450E-06 | 4.450E-06 | 4.450E-06 | 4.450E-06 | 4.450E-06 | 4.450E-06 | 4.450E-06 | 4.450E-06 | 4.450E-06 | 4.450E-06 | 4.450E-06 |
| Final [Sr] (M) | 4.180E-06 | 4.124E-06 | 3.988E-06 | 4.098E-06 | 2.023E-06 | 2.019E-06 | 1.493E-06 | 1.644E-06 | 2.754E-06 | 2.568E-06 | 3.661E-06 | 3.512E-06 | 4.168E-06 | 4.223E-06 | 3.912E-06 | 3.837E-06 |
| DF = Init/Final | 1.065E+00 | 1.079E+00 | 1.116E+00 | 1.086E+00 | 2.200E+00 | 2.204E+00 | 2.981E+00 | 2.706E+00 | 1.616E+00 | 1.733E+00 | 1.215E+00 | 1.267E+00 | 1.068E+00 | 1.054E+00 | 1.138E+00 | 1.160E+00 |
| % Removal | 6.06% | 7.34% | 10.38% | 7.91% | 54.54% | 54.63% | 66.45% | 63.05% | 38.11% | 42.28% | 17.73% | 21.07% | 6.34% | 5.11% | 12.09% | 13.78% |
| ID Number | A5-1 | A5-2 | B5-1 | B5-2 | C5-1 | C5-2 | D5-1 | D5-2 | E5-1 | E5-2 | F5-1 | F5-2 | G5-1 | G5-2 | H5-1 | H5-2 |
| Material | 3M #2999-14 CoHex unmlled | | 3M #2999-14 CoHex milled | | TAMU #TSP-137 | | TAMU #E-B Pharm-1 | | TAMU #E-B Pharm-2 | | TAMU #Phlogopite 90% Na+ | | TAMU Biotite 60% Na+ | | AS #8212-32A Zr-Biotite | |
| Kd Value | 2.209E+03 | 1.920E+03 | 2.624E+03 | 2.068E+03 | 7.784E+04 | 6.116E+04 | 4.861E+04 | 3.513E+04 | 1.992E+04 | 2.208E+04 | 3.529E+03 | 3.670E+03 | 1.653E+03 | 1.699E+03 | 2.451E+03 | 2.830E+03 |
| Load, mmol/g | 7.966E-03 | 7.167E-03 | 9.309E-03 | 7.666E-03 | 3.773E-02 | 3.888E-02 | 4.117E-02 | 3.612E-02 | 3.769E-02 | 3.939E-02 | 1.210E-02 | 1.241E-02 | 6.397E-03 | 6.532E-03 | 9.072E-03 | 1.017E-02 |
| Init [Sr] m/l | 4.450E-06 | 4.450E-06 | 4.450E-06 | 4.450E-06 | 4.450E-06 | 4.450E-06 | 4.450E-06 | 4.450E-06 | 4.450E-06 | 4.450E-06 | 4.450E-06 | 4.450E-06 | 4.450E-06 | 4.450E-06 | 4.450E-06 | 4.450E-06 |
| Fin [Sr] m/l | 3.607E-06 | 3.733E-06 | 3.548E-06 | 3.707E-06 | 4.847E-07 | 6.357E-07 | 8.468E-07 | 1.028E-06 | 1.892E-06 | 1.784E-06 | 3.428E-06 | 3.381E-06 | 3.869E-06 | 3.844E-06 | 3.702E-06 | 3.592E-06 |
| DF = Init/Fin | 1.234E+00 | 1.192E+00 | 1.254E+00 | 1.201E+00 | 9.181E+00 | 7.000E+00 | 5.255E+00 | 4.329E+00 | 2.352E+00 | 2.494E+00 | 1.298E+00 | 1.316E+00 | 1.150E+00 | 1.150E+00 | 1.202E+00 | 1.239E+00 |
| % Removal | 18.95% | 16.11% | 20.28% | 16.71% | 89.11% | 85.71% | 80.97% | 76.90% | 57.48% | 59.90% | 22.97% | 24.03% | 13.07% | 13.62% | 16.81% | 19.27% |
| ID Number | A6-1 | A6-2 | B6-1 | B6-2 | C6-1 | C6-2 | D6-1 | D6-2 | E6-1 | E6-2 | F6-1 | F6-2 | G6-1 | G6-2 | H6-1 | H6-2 |
| Material | 3M #2999-14 CoHex unmlled | | 3M #2999-14 CoHex milled | | TAMU #TSP-137 | | TAMU #E-B Pharm-1 | | TAMU #E-B Pharm-2 | | TAMU #Phlogopite 90% Na+ | | TAMU Biotite 60% Na+ | | AS #8212-32A Zr-Biotite | |
| Kd Value | 2.170E+03 | 2.649E+03 | 2.713E+03 | 2.259E+03 | 1.298E+05 | 2.683E+05 | 3.837E+04 | 3.650E+04 | 1.091E+04 | 1.623E+04 | 2.521E+03 | 3.514E+03 | 7.290E+02 | 3.131E+02 | 3.060E+03 | 2.917E+03 |
| Load, mmol/g | 7.908E-03 | 9.350E-03 | 9.562E-03 | 8.147E-03 | 4.100E-02 | 4.336E-02 | 3.823E-02 | 3.766E-02 | 2.734E-02 | 3.539E-02 | 9.138E-03 | 1.210E-02 | 3.045E-03 | 1.357E-03 | 1.094E-02 | 1.042E-02 |
| Init [Sr] m/l | 4.450E-06 | 4.450E-06 | 4.450E-06 | 4.450E-06 | 4.450E-06 | 4.450E-06 | 4.450E-06 | 4.450E-06 | 4.450E-06 | 4.450E-06 | 4.450E-06 | 4.450E-06 | 4.450E-06 | 4.450E-06 | 4.450E-06 | 4.450E-06 |
| Fin [Sr] m/l | 3.645E-06 | 3.530E-06 | 3.524E-06 | 3.606E-06 | 3.158E-07 | 1.616E-07 | 9.963E-07 | 1.032E-06 | 2.507E-06 | 2.180E-06 | 3.624E-06 | 3.444E-06 | 4.183E-06 | 4.333E-06 | 3.574E-06 | 3.572E-06 |
| DF = Init/Fin | 1.221E+00 | 1.261E+00 | 1.263E+00 | 1.234E+00 | 1.409E+01 | 2.754E+01 | 4.467E+00 | 4.313E+00 | 1.775E+00 | 2.041E+00 | 1.228E+00 | 1.292E+00 | 1.064E+00 | 1.027E+00 | 1.245E+00 | 1.246E+00 |
| % Removal | 18.10% | 20.68% | 20.81% | 18.96% | 92.90% | 96.37% | 77.61% | 76.81% | 43.67% | 51.01% | 18.56% | 22.60% | 6.01% | 2.62% | 19.68% | 19.72% |
| ID Number | A7-1 | A7-2 | B7-1 | B7-2 | C7-1 | C7-2 | D7-1 | D7-2 | E7-1 | E7-2 | F7-1 | F7-2 | G7-1 | G7-2 | H7-1 | H7-2 |
| Material | 3M #2999-14 CoHex unmlled | | 3M #2999-14 CoHex milled | | TAMU #TSP-137 | | TAMU #E-B Pharm-1 | | TAMU #E-B Pharm-2 | | TAMU #Phlogopite 90% Na+ | | TAMU Biotite 60% Na+ | | AS #8212-32A Zr-Biotite | |
| Kd Value | 2.654E+03 | 2.710E+03 | 2.630E+03 | 2.824E+03 | 2.450E+05 | 1.053E+05 | 5.530E+04 | 4.460E+04 | 1.949E+04 | 1.715E+04 | 3.797E+03 | 3.527E+03 | 1.015E+03 | 8.872E+02 | 3.150E+03 | 3.777E+03 |
| Load, mmol/g | 9.317E-03 | 9.406E-03 | 9.228E-03 | 9.866E-03 | 4.103E-02 | 3.840E-02 | 4.185E-02 | 4.066E-02 | 3.760E-02 | 3.455E-02 | 1.276E-02 | 1.195E-02 | 4.134E-03 | 3.650E-03 | 1.116E-02 | 1.312E-02 |
| Init [Sr] m/l | 4.450E-06 | 4.450E-06 | 4.450E-06 | 4.450E-06 | 4.450E-06 | 4.450E-06 | 4.450E-06 | 4.450E-06 | 4.450E-06 | 4.450E-06 | 4.450E-06 | 4.450E-06 | 4.450E-06 | 4.450E-06 | 4.450E-06 | 4.450E-06 |
| Fin [Sr] m/l | 3.511E-06 | 3.471E-06 | 3.508E-06 | 3.494E-06 | 1.675E-07 | 3.646E-07 | 7.569E-07 | 9.116E-07 | 1.917E-06 | 2.014E-06 | 3.360E-06 | 3.388E-06 | 4.074E-06 | 4.114E-06 | 3.542E-06 | 3.475E-06 |
| DF = Init/Fin | 1.268E+00 | 1.282E+00 | 1.268E+00 | 1.274E+00 | 2.657E+01 | 1.220E+01 | 5.880E+00 | 4.881E+00 | 2.321E+00 | 2.209E+00 | 1.324E+00 | 1.314E+00 | 1.092E+00 | 1.082E+00 | 1.256E+00 | 1.280E+00 |
| % Removal | 21.10% | 22.00% | 21.16% | 21.49% | 96.24% | 91.81% | 82.99% | 79.51% | 56.92% | 54.73% | 24.49% | 23.87% | 8.45% | 7.55% | 20.41% | 21.90% |
| ID Number | A8-1 | A8-2 | B8-1 | B8-2 | C8-1 | C8-2 | D8-1 | D8-2 | E8-1 | E8-2 | F8-1 | F8-2 | G8-1 | G8-2 | H8-1 | H8-2 |
| Material | 3M #2999-14 CoHex unmlled | | 3M #2999-14 CoHex milled | | TAMU #TSP-137 | | TAMU #E-B Pharm-1 | | TAMU #E-B Pharm-2 | | TAMU #Phlogopite 90% Na+ | | TAMU Biotite 60% Na+ | | AS #8212-32A Zr-Biotite | |
| Kd Value | 1.110E+03 | 1.019E+03 | 1.126E+03 | 1.276E+03 | 2.076E+05 | 2.167E+05 | 4.329E+04 | 3.105E+04 | 1.781E+04 | 1.733E+04 | 2.704E+03 | 1.398E+03 | 4.509E+02 | 5.374E+02 | 2.430E+03 | 2.593E+03 |
| Load, mmol/g | 4.426E-03 | 4.105E-03 | 4.491E-03 | 5.042E-03 | 4.250E-02 | 4.227E-02 | 3.903E-02 | 3.601E-02 | 3.608E-02 | 3.502E-02 | 9.766E-03 | 5.525E-03 | 1.927E-03 | 2.279E-03 | 8.999E-03 | 9.497E-03 |
| Init [Sr] m/l | 4.450E-06 | 4.450E-06 | 4.450E-06 | 4.450E-06 | 4.450E-06 | 4.450E-06 | 4.450E-06 | 4.450E-06 | 4.450E-06 | 4.450E-06 | 4.450E-06 | 4.450E-06 | 4.450E-06 | 4.450E-06 | 4.450E-06 | 4.450E-06 |
| Fin [Sr] m/l | 3.988E-06 | 4.029E-06 | 3.989E-06 | 3.953E-06 | 2.048E-07 | 1.951E-07 | 9.015E-07 | 1.160E-06 | 2.035E-06 | 2.021E-06 | 3.410E-06 | 3.951E-06 | 4.275E-06 | 4.241E-06 | 3.703E-06 | 3.662E-06 |
| DF = Init/Fin | 1.116E+00 | 1.105E+00 | 1.115E+00 | 1.126E+00 | 2.173E+01 | 2.281E+01 | 4.936E+00 | 3.837E+00 | 2.186E+00 | 2.202E+00 | 1.232E+00 | 1.126E+00 | 1.041E+00 | 1.049E+00 | 1.202E+00 | 1.215E+00 |
| % Removal | 10.38% | 9.47% | 10.35% | 11.17% | 95.40% | 95.62% | 79.74% | 73.94% | 54.26% | 54.58% | 18.85% | 11.22% | 3.94% | 4.70% | 16.78% | 17.70% |
| ID Number | A9-1 | A9-2 | B9-1 | B9-2 | C9-1 | C9-2 | D9-1 | D9-2 | E9-1 | E9-2 | F9-1 | F9-2 | G9-1 | G9-2 | H9-1 | H9-2 |
| Material | 3M #2999-14 CoHex unmlled | | 3M #2999-14 CoHex milled | | TAMU #TSP-137 | | TAMU #E-B Pharm-1 | | TAMU #E-B Pharm-2 | | TAMU #Phlogopite 90% Na+ | | TAMU Biotite 60% Na+ | | AS #8212-32A Zr-Biotite | |
| Kd Value | 8.320E+02 | 7.833E+02 | 8.292E+02 | 1.515E+03 | 1.510E+05 | 1.650E+05 | 3.399E+04 | 5.309E+04 | 1.830E+04 | 2.270E+04 | 2.758E+03 | 2.807E+03 | 1.958E+03 | 1.785E+03 | 3.843E+03 | 4.280E+03 |
| Load, mmol/g | 3.391E-03 | 3.228E-03 | 3.387E-03 | 5.777E-03 | 4.017E-02 | 4.066E-02 | 3.555E-02 | 3.857E-02 | 3.464E-02 | 3.720E-02 | 9.784E-03 | 9.922E-03 | 7.365E-03 | 6.751E-03 | 1.288E-02 | 1.411E-02 |
| Init [Sr] m/l | 4.450E-06 | 4.450E-06 | 4.450E-06 | 4.450E-06 | 4.450E-06 | 4.450E-06 | 4.450E-06 | 4.450E-06 | 4.450E-06 | 4.450E-06 | 4.450E-06 | 4.450E-06 | 4.450E-06 | 4.450E-06 | 4.450E-06 | 4.450E-06 |
| Fin [Sr] m/l | 4.075E-06 | 4.122E-06 | 4.084E-06 | 3.813E-06 | 4.660E-07 | 2.465E-07 | 1.048E-06 | 7.265E-07 | 1.893E-06 | 1.639E-06 | 3.547E-06 | 3.534E-06 | 3.761E-06 | 3.782E-06 | 3.352E-06 | 3.298E-06 |
| DF = Init/Fin | 1.092E+00 | 1.080E+00 | 1.090E+00 | 1.187E+00 | 1.673E+01 | 1.805E+01 | 4.256E+00 | 6.125E+00 | 2.351E+00 | 2.716E+00 | 1.255E+00 | 1.259E+00 | 1.183E+00 | 1.177E+00 | 1.327E+00 | 1.349E+00 |
| % Removal | 8.43% | 7.38% | 8.22% | 14.31% | 94.02% | 94.46% | 76.50% | 83.67% | 57.46% | 63.18% | 20.29% | 20.58% | 15.48% | 15.01% | 24.66% | 25.89% |
| ID Number | A0-1 | A0-2 | B0-1 | B0-2 | C0-1 | C0-2 | D0-1 | D0-2 | E0-1 | E0-2 | F0-1 | F0-2 | G0-1 | G0-2 | H0-1 | H0-2 |
| Material | 3M #2999-14 CoHex unmlled | | 3M #2999-14 CoHex milled | | TAMU #TSP-137 | | TAMU #E-B Pharm-1 | | TAMU #E-B Pharm-2 | | TAMU #Phlogopite 90% Na+ | | TAMU Biotite 60% Na+ | | AS #8212-32A Zr-Biotite | |
| Kd Value | 9.700E+02 | 7.789E+02 | 8.398E+02 | 1.150E+03 | 3.120E+04 | 3.397E+04 | 2.128E+04 | 9.261E+03 | 1.001E+04 | 1.150E+04 | 1.576E+03 | 1.438E+03 | 1.071E+03 | 1.831E+03 | 2.203E+03 | 1.981E+03 |
| Load, mmol/g | 3.924E-03 | 3.211E-03 | 3.443E-03 | 4.597E-03 | 3.268E-02 | 3.273E-02 | 3.240E-02 | 2.251E-02 | 2.694E-02 | 2.911E-02 | 6.222E-03 | 5.696E-03 | 4.341E-03 | 6.956E-03 | 8.330E-03 | 7.593E-03 |
| Init [Sr] m/l | 4.450E-06 | 4.450E-06 | 4.450E-06 | 4.450E-06 | 4.450E-06 | 4.450E-06 | 4.450E-06 | 4.450E-06 | 4.450E-06 | 4.450E-06 | 4.450E-06 | 4.450E-06 | 4.450E-06 | 4.450E-06 | 4.450E-06 | 4.450E-06 |
| Fin [Sr] m/l | 4.046E-06 | 4.122E-06 | 4.100E-06 | 3.989E-06 | 4.043E-06 | 4.635E-07 | 1.523E-06 | 4.431E-06 | 2.683E-06 | | | | | | | |

Distribution

No. of
Copies

No. of
Copies

OFFSITE

| | | | |
|---|---|--|--|
| | D. H. Bandy U.S. Department of Energy P.O. Box 5400 Albuquerque, NM 87115 | | J. Coronas Ames Laboratory 329 Wilhelm Hall Iowa State University Ames, IA 50011 |
| | J. E. Baublitz, EM-40 DOE/Office of Environmental Restoration Forrestal Building U.S. Department of Energy 1000 Independence Ave. SW Washington, DC 20585 | | R. Craig HAZWRAP P.O. Box 2003, MS 7606 Oak Ridge, TN 37831-7606 |
| | J. P. Bibler Westinghouse Savannah River Co. Building 773 A Aiken, SC 29802 | | 6 DOE/Office of Science and Technology Trevion II Building 12800 Middlebrook Road Germantown, MD 20874 ATTN: G. G. Boyd EM-50 S. T. Lien EM-53 R. T. Parker EM-52 P. J. Ritzcovan EM-542 W. C. Schutte EM-54 S. M. Wolfe EM-532 |
| 2 | W. W. Bixby, EM-60 DOE/Office of the Deputy Assistant Secretary Facility Transition and Management U.S. Department of Energy 1000 Independence Ave. SW Washington, DC 20585 | | 4 DOE/Office of Waste Management Trevion II Building 12800 Middlebrook Road Germantown, MD 20874 ATTN: J. O. Boda EN-32 J. A. Coleman EM-35 S. L. Domotor EM-35 H. F. Walter EM-34 |
| | N. E. Brown 6608 Loftus, NE Albuquerque, NM 87109 | | |
| | R. L. Bruening 505 East 1860 South IBC Advanced Technologies, Inc. American Fork, UT 84603 | | N. Egan Program Development Division MSE Inc. P.O. Box 3767 Butte, MT 59702 |

No. of
CopiesNo. of
Copies

| | | | |
|---|--|--|---|
| | D. Emilia Strategic Planning Dept. Chem-Nuclear Geotech P.O. Box 1400 2597B-3/4 Road (81503) Grand Junction, CO 81502-2567 | | J. E. Helt Office of Waste Management Programs 9700 South Cass Avenue Argonne, IL 60439-4837 |
| | B. Erdal Los Alamos National Laboratory MS D446 Los Alamos, NM 87545 | | R. Jacobson Desert Research Institute P.O. Box 19040 Las Vegas, NV 89132 |
| | D. J. Fennelly UOP Corp. 307 Fellowship Road Suite 207 Mt. Laurel, NJ 08054 | | 3 T. M. Kafka 3M Center Bldg. 209-1W-24 St. Paul, MN 55144-1000 |
| 2 | J. J. Fiore, EM-42 DOE/Office of Environmental Restoration Trevion II Building 12800 Middlebrook Road Germantown, MD 20874 | | K. Kostelnik EG&G Idaho, Inc., MS 3930 P.O. Box 1625 200 South Woodruff Idaho Falls, ID 83415-3970 |
| | C. W. Frank, EM-50 DOE/Office of Technology Development Forrestal Building U.S. Department of Energy 1000 Independence Ave. SW Washington, DC 20585 | | J. E. Lytle, EM-30 DOE/Office of Waste Operations Forrestal Building U.S. Department of Energy 1000 Independent Ave. SW Washington, DC 20585 |
| | E. Franz Brookhaven National Laboratory Building 830 Upton, NY 11973 | | J. F. McGlynn SAIC 555 Quince Orchard Road, Suite 500 Gaithersburg, MD 20878 |
| | K. D. Gerdes, EM-532 DOE/Office of Technology Development 19901 Germantown Road Germantown, MD 20874 | | Frances Fadullon SAIC 555 Quince Orchard Road, Suite 500 Gaithersburg, MD 20878 |

No. of
Copies

No. of
Copies

| | | | |
|---|--|---|--|
| | K. McWilliam U.S. Department of Energy Nevada Operations Office P.O. Box 98518 Las Vegas, NV 89109 | | P. J. Pettit P.O. Box 538704 Mailstop 81-2 Cincinnati, OH 45253-8704 |
| | J. Moore U.S. Department of Energy Oak Ridge Operations Office P.O. Box E Oak Ridge, TN 37831 | | R. W. Rice MSE, Inc. 307 Quincy El Paso, TX 79922 |
| 9 | Oak Ridge National Laboratory P.O. Box 2008 Oak Ridge, TN 37831-6223 ATTN: Lockheed Martin Hanford G3-21 | 3 | Sandia National Laboratories P.O. Box 5800 Albuquerque, NM 87185-5800 ATTN: J. E. Miller J. Nelson G. Allen |
| | J. L. Collins MS-6221 B. Z. Egan MS-6223 R. D. Hunt MS-6273 D. Lee MS-6221 A. P. Malinauskas MS-7271 C. P. McGinnis MS-6273 J. F. Walker MS-6149 J. S. Watson MS-6149 | | G. Staats U.S. Department of Energy Pittsburgh Energy Technology Center P.O. Box 10940 Pittsburgh, PA 15236-0940 |
| | D. Olona U.S. Department of Energy Albuquerque Operations Office P.O. Box 5400 Albuquerque, NM 87115 | | J. L. Steele Savannah River Site SRL, 733 A, A208 Aiken, SC 29802 |
| | B. Park MSE Inc. P.O. Box 4078 Butte, MT 59702 | | J. L. Swanson 1318 Cottonwood Drive Richland, WA 99352 |
| | J. Tourikis MSE Inc. P.O. Box 4078 Butte, MT 59702 | | J. Sweeney U.S. Department of Energy Oak Ridge Operations Office P.O. Box E Oak Ridge, TN 37831 |

No. of
Copies

No. of
Copies

I. R. Tasker
Waste Policy Institute
Quince Diamond Executive Center
555 Quince Orchard Road
Gaithersburg, MD 20878-1437

M. C. Thompson
Savannah River Technology Center
P.O. Box 616
Aiken, SC 29802

T. A. Todd
Lockheed Idaho Technology Company
P.O. Box 1625, MS 5213
Idaho Falls, ID 83415

C. Tsang
Earth Sciences Division
Bldg, 50E
Lawrence Berkeley Laboratory
Berkeley, CA 94720

UOP Corp.
50 East Algonquin
Des Plaines, IL 60017-5016
ATTN: J. Sherman
R. Braun

S. Webster
U.S. Department of Energy
Chicago Field Office
9800 South Cass Avenue
Argonne, IL 60439-4837

T. Williams
U.S. Department of Energy
Idaho Operations Office
785 DOE Place
Idaho Falls, ID 83402

J. Wright
U.S. Department of Energy
Savannah River Operations Office
RFD #1, Bldg. 703A, Rm. E208 North
P.O. Box A
Aiken, SC 29802

S. Yates
Allied Signal
50 East Algonquin Road
Des Plaines, IL 60017-5016

J. Yow
Lawrence Livermore National Laboratory
7000 East Avenue
P.O. Box 808
Livermore, CA 94550

C. Zeh
Morgantown Energy Technology Center
3610 Collins Ferry Road
Morgantown, WV 26507-0880

ONSITE

9 DOE Richland Operations Office

| | |
|---------------|-------|
| N. R. Brown | K6-51 |
| J. A. Frey | K8-50 |
| R. A. Gilbert | K6-51 |
| J. P. Hanson | K8-50 |
| P. E. Lamont | S7-53 |
| C. S. Louie | S7-53 |
| B. M. Mauss | K8-50 |
| D. E. Trader | K8-50 |
| L. F. Waldorf | K6-51 |

